Chapter 6

Stereolithographic 3D Bioprinting for Biomedical Applications

Ritu Raman[*,‡] and Rashid Bashir[**,†,‡]

[*]*Department of Mechanical Science and Engineering, University of Illinois at Urbana-Champaign, Urbana, IL, USA;* [**]*Department of Bioengineering, University of Illinois at Urbana-Champaign, Urbana, IL, USA;* [†]*Department of Electrical and Computer Engineering, University of Illinois at Urbana-Champaign, Urbana, IL, USA;* [‡]*Micro and Nanotechnology Laboratory, University of Illinois at Urbana-Champaign, Urbana, IL, USA*

Chapter Outline

Essentials of 3D Biofabrication and Translation. http://dx.doi.org/10.1016/B978-0-12-800972-7.00006-2

ABSTRACT

In recent years, stereolithographic fabrication has advanced greatly in the quality, resolution, and accuracy of manufactured parts. The concurrent development of photocurable resins that are biocompatible, biodegradable, and bioactive has enabled a vast array of biomedical and translation medical applications of stereolithography-based fabrication technologies. Stereolithographic techniques have been readily integrated with medical imaging technologies in order to improve disease diagnosis, preoperative planning, quality and morphology of prosthetics and implants, and functional success of complex surgeries. Furthermore, stereolithography has established itself as one of the primary enabling tools that will be useful for regenerative medicine applications in the coming years. As a whole, the versatility in design, scale, resolution, and broad applicability of stereolithographic technologies render them the ideal enabling technology for biomedical and translational medical applications.

Keywords: stereolithography; prosthetics; implants; tissue engineering; regenerative medicine

1 INTRODUCTION

Stereolithographic 3D printing is a solid freeform additive layer manufacturing technology that was pioneered by the 3D Systems manufacturing company in 1986. Originally intended for use in rapid prototyping for manufacturing sectors, such as the automotive and aeronautic industries, stereolithography revolutionized this field by eliminating the need for inefficient and expensive methods of manufacture. As the first commercially available and most popular form of solid freeform fabrication technology, stereolithography has undergone decades of further developments in efficiency and accuracy, yielding surface finish quality comparable to traditional machine milling and rendering it one of the most commercially viable additive manufacturing technologies available at present. The many advancements in this field and the advantages associated with this versatile manufacturing technology thus encourage its widespread use and adaptation to a variety of industry sectors, most interestingly applications in biomedical and translational research [1].

Stereolithography demonstrates greater versatility in scale of fabricated parts (submicron to decimeter) and has the highest fabrication accuracy and resolution as compared to other additive layer manufacturing technologies [2]. Alternative additive manufacturing apparatus, such as selective laser sintering (SLS), sheet lamination (LOM), or adhesion bonding (3DP) machines, are restricted to fabricating parts with less complex internal geometries because they are limited by unused material being trapped inside internal holes. Fused deposition modeling (FDM) apparatus, like SLA, are not limited by this, but do have high heat effects on the raw material used for fabrication [3]. The cost of fabricating parts via stereolithography is comparable to other additive manufacturing apparatus and is counterbalanced by the versatility of design, high resolution, and superior quality of parts fabricated via SLA [4].

The main limitation facing the advancement of stereolithography for translational biomedical applications is the scarcity of suitable biocompatible and biodegradable photopolymerizable liquid polymer resins. As shall be seen in this chapter, this limitation is being daily reduced by the development of a vast array of stereolithographic resin materials including families of natural and synthetic polymers, ceramics, composites, hydrogels, and even living cells. These resins have been altered and tuned to target a myriad array of biomedical applications.

This chapter outlines the use of stereolithographic manufacturing processes to fabricate a variety of models and structures that have translational applications in biomedical engineering. Section 2 introduces the physics and materials chemistry governing the stereolithographic fabrication process, with special emphasis placed on the design challenges pertinent to biofabrication applications. Section 3 elaborates on applications of stereolithographic fabrication in surgical procedures, prosthesis, and implants, introducing concepts that promise to improve upon currently existing clinical practices that are in wide use and operation. Section 4 covers the use of stereolithography to fabricate biomaterial scaffolds and tissue substitutes for novel and rapidly evolving applications in tissue engineering and regenerative medicine. A discussion of the current challenges present in the field of stereolithography, as well as the anticipated advancements in this field, is presented in Section 5. A presentation of stereolithographic biofabrication in the broader context of translational 3D biofabrication and a discussion of future research trends concludes this chapter.

2 THE STEREOLITHOGRAPHIC PROCESS

Stereolithographic systems rely on the process of photopolymerization, or light-initiated polymerization, to fabricate 3D structures. In general, stereolithographic processes can be separated into two broad categories: single-photon and multiphoton methods, which differ in the method of light excitation and absorption that trigger the polymerization process. Single-photon methods can be further divided into: (1) Visible radiation systems that employ light in the visible wavelength range; (2) "Conventional" stereolithography systems that employ ultraviolet (UV) radiation; (3) IR stereolithography systems that employ infrared (IR) radiation; (4) Stereo-thermal lithography systems that combine UV and IR radiation to initiate polymerization [5]. All these single-photon polymerization processes can be implemented using direct-laser writing, physical mask projection, or digital mask projection machines, as shall be described in later sections. Of the diverse array of stereolithographic systems just listed,

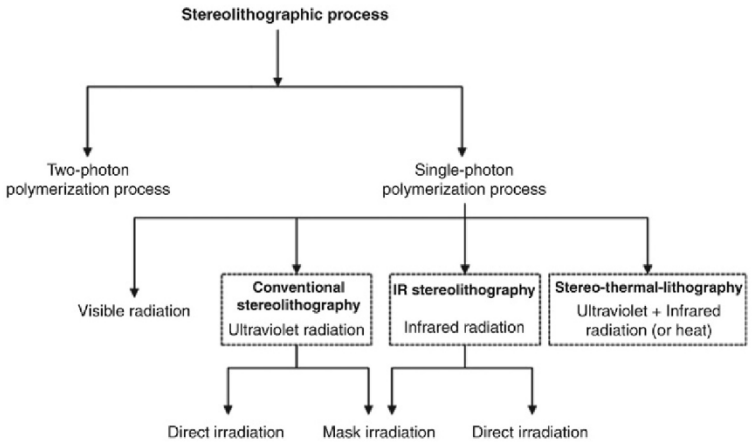

FIGURE 6.1 Broad categorization of the forms of stereolithographic processes into single-photon and multiphoton methods. Single-photon methods, which are the most commonly employed for translational biomedical applications, can be implemented using several forms of excitation radiation [5].

conventional single-photon stereolithography apparatus (SLA) are by far the most popular (Fig. 6.1).

Conventional SLA machines utilize the energy from an UV light source to drive the conversion of UV-irradiation-sensitive liquid oligomers into cross-linked solid/gel-like polymeric networks. These machines, as well as SLA machines based on visible light irradiation, possess the advantage of providing precise spatial and temporal control of reaction kinetics as they are governed purely by the ease of light manipulation. Recent advances in developing controlled light sources, such as lasers, have thus greatly enhanced the advantages of using such systems. Conventional stereolithography systems have likewise seen the greatest use and adaption in biomedical and translational research, as they have the ability to drive polymerization under physiologic conditions with minimal heat production and damage to the raw material. This is of special relevance in 3D fabrication of structures containing encapsulated living cells, as discussed in Section 4.

As with most additive layer manufacturing technologies, the first step in fabricating a 3D structure by stereolithography involves creating a digital model of the part, using computer-aided design software (CAD). Lately, advanced digital scanners have also been used to convert complex structures into virtual 3D models. This is of special interest in the context of biomedical and translational applications, as many of the scanning technologies that are used in this field have their basis in clinical imaging technologies such as magnetic resonance imaging (MRI) and computed tomography (CT). Complex structures, such as those found inside the human body, can thus be imaged and readily converted into 3D digital models for manufacturing patient-specific models, implants, and tissue-engineered replacements for damaged tissue.

In order to be prepared for 3D printing, all digital models must first be converted to a standard tessellation language file format (STL) that represents the surface geometry of the 3D model as a series of interconnecting tessellated triangles. Specialized software is then used to virtually slice the model into sequential layers of specified thickness, often determined by the user-specified part size, required resolution, and desired accuracy of the final part. The resulting information is then sent to the stereolithography apparatus, which builds the 3D model layer-by-layer sequentially from the bottom up. Schematics of various forms of SLA machines are further described in Section 2.1 (Figs 6.2 and 6.3).

2.1 Stereolithographic Fabrication Apparatus

2.1.1 *Single-Photon Stereolithography*

Single-photon stereolithographic fabrication processes are so termed because the process of photoinitiator excitation in this process is driven by the absorption of a single photon. Conventional UV light-based stereolithography falls under this category of photopolymerization, as does visible light-based stereolithography. The two most basic and widely adopted apparatus for single-photon photolithography in the context of biomedical applications are direct laser writing and mask-based UV light-based stereolithography.

A direct laser writing stereolithographic apparatus uses a high-energy laser to trace lines across the resin surface, serially polymerizing (i.e., "rasterizing") two-dimensional cross-sections of a three-dimensional design. Sequential polymerization of these two-dimensional cross-sections layer by layer from the bottom up, with the aid of a computer-controlled stage, drives formation of three-dimensional structures [5].

Similarly, mask-based stereolithography filters a high-energy light source through a patterned physical or digital mask, allowing for curing of an entire two-dimensional

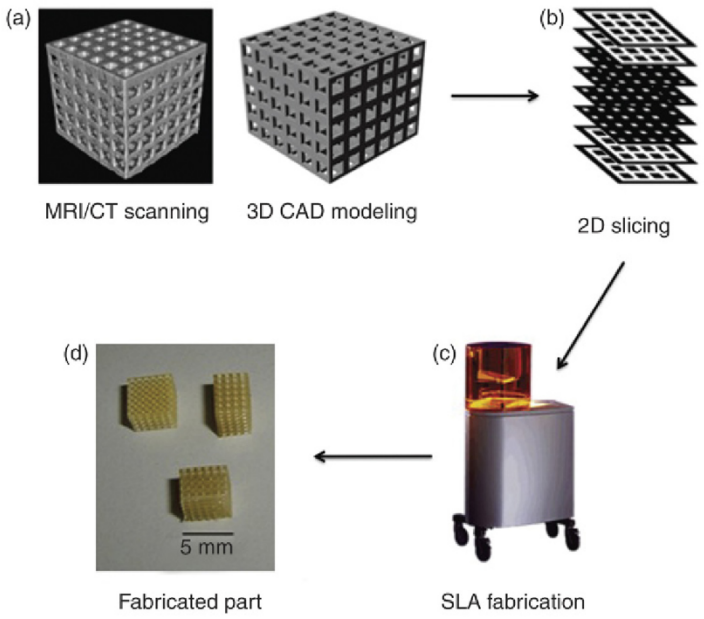

FIGURE 6.2 Process flow for fabricating 3D parts via stereolithography. (a) Scanning to create a 3D digital image of a design or creating a 3D solid model via computer-aided design software (CAD); (b) digitally slicing the 3D model layer-by-layer into 2D sections; (c) fabricating the 3D model layer-by-layer using a stereolithographic apparatus; (d) the final fabricated part with the desired feature sizes, scale, resolution, and surface finish [1].

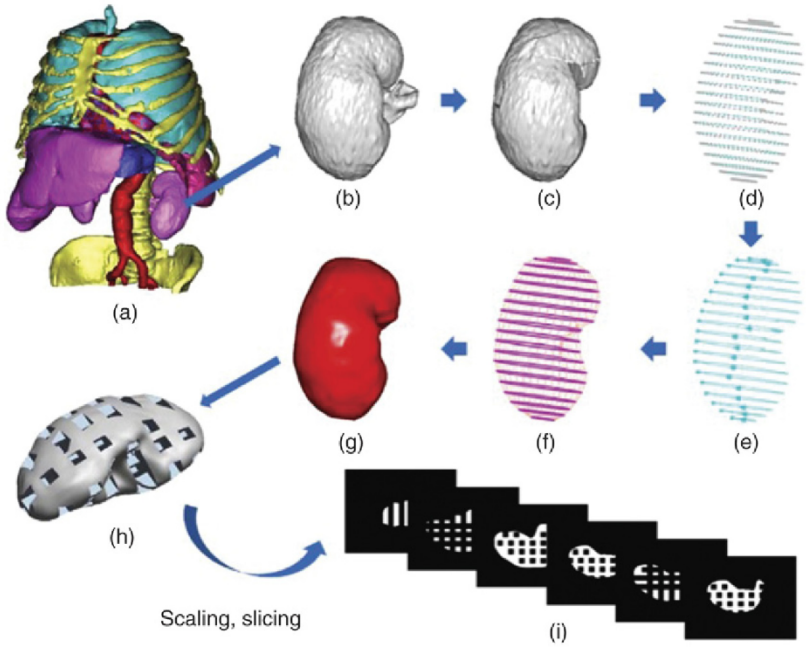

FIGURE 6.3 Digital scanning of biological tissues with complex 3D structures is a multistep process. (a) CT imaging data are gathered; (b) point cloud data are extracted from scan using reverse engineering software; (c) point cloud data are "cleaned" to remove imaging noise/defects; (d) point cloud is sliced into 2D cross-sections; (e) point cloud layers are converted into spline curves; (f) a lofted surface is created from the splines; (g) a solid geometry model of the biological tissue is created; (h) the solid model is converted into a porous scaffold for applications in tissue engineering and regenerative medicine; (i) the porous model is scaled sliced into 2D layers and sent to an SLA machine for fabrication [36].

cross-section within a single exposure, rather than serially tracing lines as with a laser-based apparatus. This process is thus considered higher-throughput than laser-based processes, as complete layers of resin can be polymerized within a single light exposure, thereby reducing build-time. It is of importance to remember, however, that resolution of feature sizes obtainable via mask-based projection stereolithography systems is inversely proportional to the size/scale of

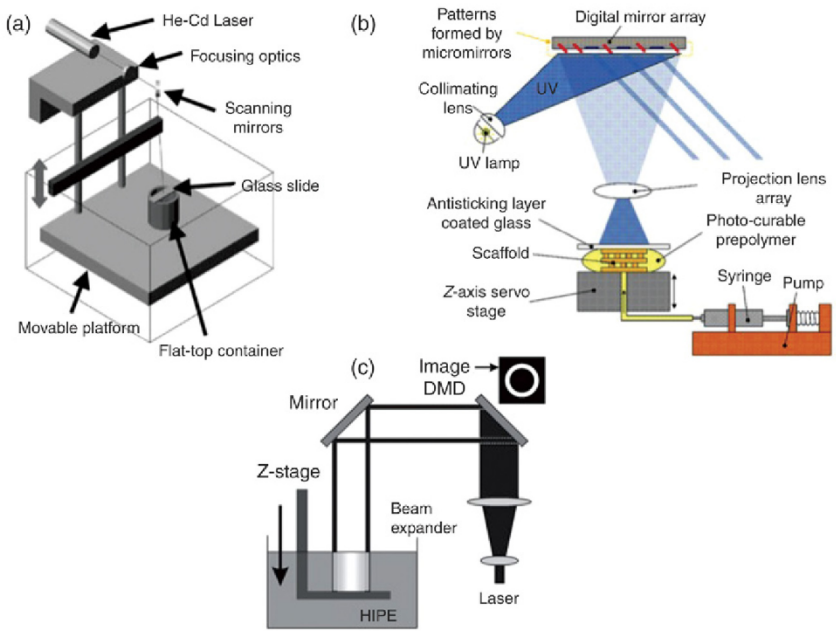

FIGURE 6.4 Schematic of (a) laser-based SLA that directly "writes" patterns in photopolymerizable resin by serially tracing 2D cross-sections of 3D designs [41]; (b) mask-based SLA that polymerizes 2D cross-sections in a single projection to create 3D designs layer-by-layer [49]; (c) schematic of SLA that combines a laser light source and digital micromirror mask device to fabricate large-scale 3D parts with complex and high-resolution features [6].

the final manufactured part. Hence, fabricating large parts with very small feature sizes can be a time-consuming process, as it will require rasterizing several 2D projections to completely polymerize an entire 2D cross-section of the 3D model. Novel SLA that employ a combination of a laser light source and mask-based projection system have been developed to target this mismatch between part size, resolution, and fabrication time, but these apparatus are yet to be widely employed [6].

Physical masks used in this type of mask-based projection photolithography are manufactured via the microfabrication approaches that were initially developed to target applications in semiconductor manufacturing. Greater design flexibility is enabled by the use of digital masks that can display a vast array of different patterns. One of the most commonly used digital masks used in this type of stereolithography is inspired by the digital light processing technology in projectors, projection-based television sets, digital signs, and digital cinema projection. The digital mask, or digital micromirror device (DMD), is comprised of an array of millions of microscopic mirrors that can be precisely and independently rotated into an "on" state or an "off" state, generating a pixelated-pattern image. Patterning and projection of light through this digital mask enables the photopolymerization of a stereolithographic resin in precisely defined patterns [7,8].

Both laser-based and mask-based SLA rely heavily on computer-controlled building stages that move the 2D polymerized cross-sections by a precisely defined amount to ensure adherence of sequential layers to one another. Understanding of the cure depth relationship of the resin in use, as well as precise calibration of the light energy of the apparatus, is thus of great importance in manufacturing 3D parts via single-photon stereolithography (Fig. 6.4).

2.1.2 *Multiphoton Stereolithography*

Two-photon stereolithographic fabrication processes represent the simplest case of multiphoton absorption, and involve the sequential or simultaneous absorption of two relatively low-intensity photons in order to excite a photosensitive resin to a high-energy radical state. This method of excitation depends quadratically on the incident light intensity [5], as opposed to the linear relationship for single-photon stereolithography, allowing for extremely rapid fabrication in three dimensions with submicron resolution (Fig. 6.5).

In two-photon initiated stereolithography, which was first demonstrated by Kawata and coworkers in 1997 [9], femtosecond light pulses from a near-IR laser are focused into a 3D volume/vat of liquid resin. The polymerization process is initiated in the precisely defined focal volume of the laser, limiting interaction with the resin through which the laser passes to reach the focal volume. Shifting the focal plane of the laser enables the fabrication of complex three-dimensional structures with high-resolution feature sizes [10]. Similarly, three-photon approaches to photopolymerization of 3D structures with submicron resolution have also been demonstrated [11]. There is great

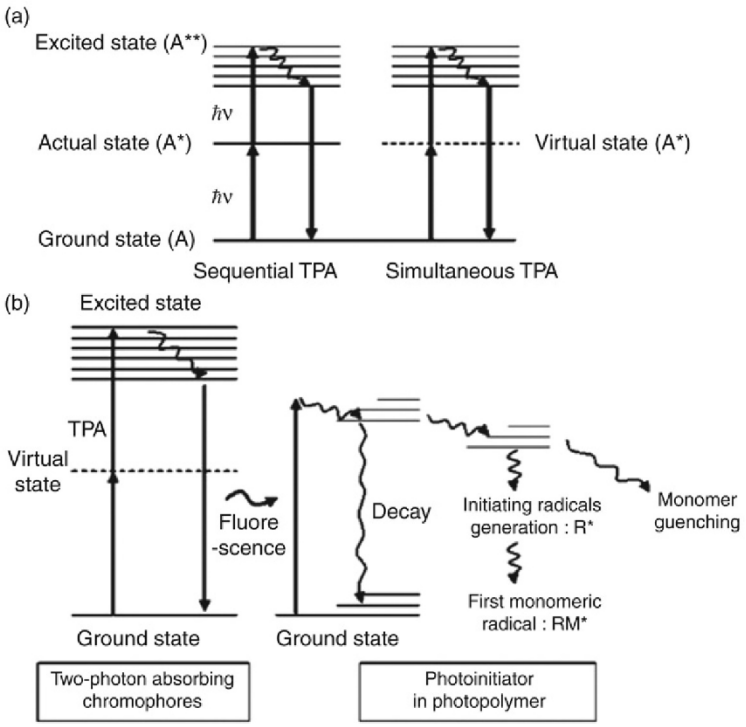

FIGURE 6.5 Multiphoton stereolithographic polymerization involves the absorption of multiple photons in order to excite a photosensitive resin to a high-energy radical state. (a) For two-photon polymerization, this high-energy radical state can be accomplished via sequential or simultaneous absorption of two photons. The energy of incident photons is represented by $h\nu$ (the product of Planck's constants divided by 2π and angular frequency of incident light, respectively). A and A* denote energy levels; (b) schematic diagrams of multiphoton-initiated polymerization showing valence electrons in a photoinitiator excited to a high-energy state and transforming by: (1) decaying back to photoinitiator with emission of light, (2) generating an excited state quenching by oxygen, or (3) yielding an initiator species for polymerization. All three competing processes are required for efficient photopolymerization [10].

potential for using multiphoton fabrication approaches to manufacture three-dimensional scaffolds with complex internal microarchitectures for tissue engineering applications [12]. Multiphoton methods for patterning living cells encapsulated within photosensitive resins have also been demonstrated [13]. It is to be noted that photoinitiators used for conventional stereolithography are often unsuitable for applications in two-photon initiated stereolithography (see Section 2.2.1), as these chemicals demonstrate reduced photosensitivity to light in the near-IR wavelength range [5] (Fig. 6.6).

2.1.3 Interference Stereolithography

A novel form of photolithography known as interference lithography (alternatively known as holography) is based on creating an interference pattern between multiple coherent light waves in order to create a pattern of high intensity and low intensity fringes of light [14]. Photosensitive resins exposed to this interference-derived pattern of light are thus polymerized in regions of high intensity fringes. This method can be used to create patterns with nanoscale resolution and offers the additional advantage of more rapid polymerization than attainable via conventional stereolithography [15]. However, because interference lithography is restricted in the number and type of patterns that can be created via light interference, it is only of interest in biomedical applications that require repetitive structures [16]. For example, tissue engineering of cancellous/trabecular bone requires the formation of an ossified "spongy" scaffold with a repetitive porous structure. This type of scaffold, and other scaffolds that require similar repetitive porous structures, could be rapidly and accurately fabricated via an interference lithography fabrication apparatus (Fig. 6.7).

2.2 Stereolithographic Resins

A conventional stereolithography single-photon photofabrication apparatus uses the energy from UV light to selectively polymerize, or "cure" photosensitive liquids called resins to form solid or gel-like structures. Photosensitive resins, which are the raw materials used in conventional stereolithography, are composed primarily of polymerizable oligomers, or "prepolymers," and a radical photoinitiator. The polymerization process of these resins can be simply described in three steps: initiation, propagation, and termination. During *initiation*, components of the resin are irradiated by light and form reactive radical species. These radicals then *propagate* between polymerizable oligomers

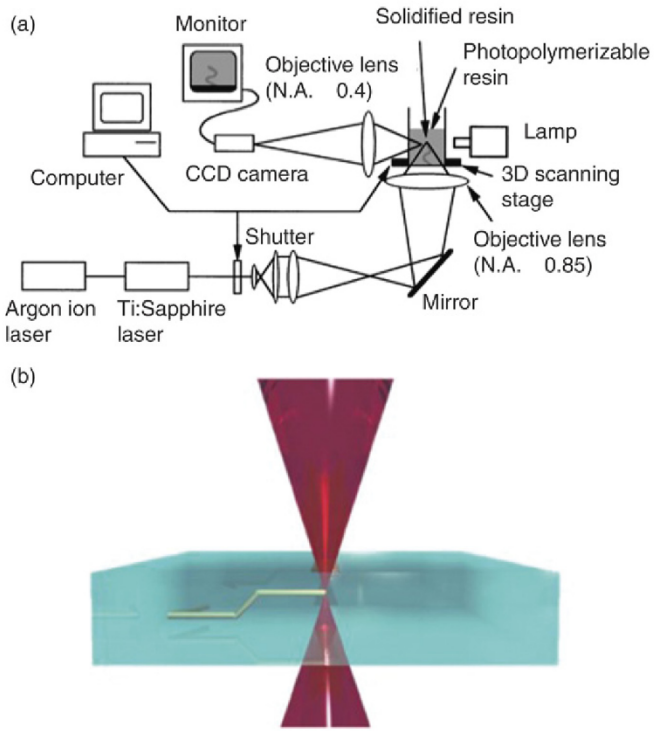

FIGURE 6.6 **Multiphoton stereolithographic apparatus.** (a) Optical system for two-photon laser-based photolithographic fabrication approach [9]; (b) polymerization occurs via tracing of femtosecond laser through 3D vat of photosensitive resin. Shifting the plane of laser focus shifts the plane of polymerization, enabling high-resolution fabrication of complex 3D structures [13].

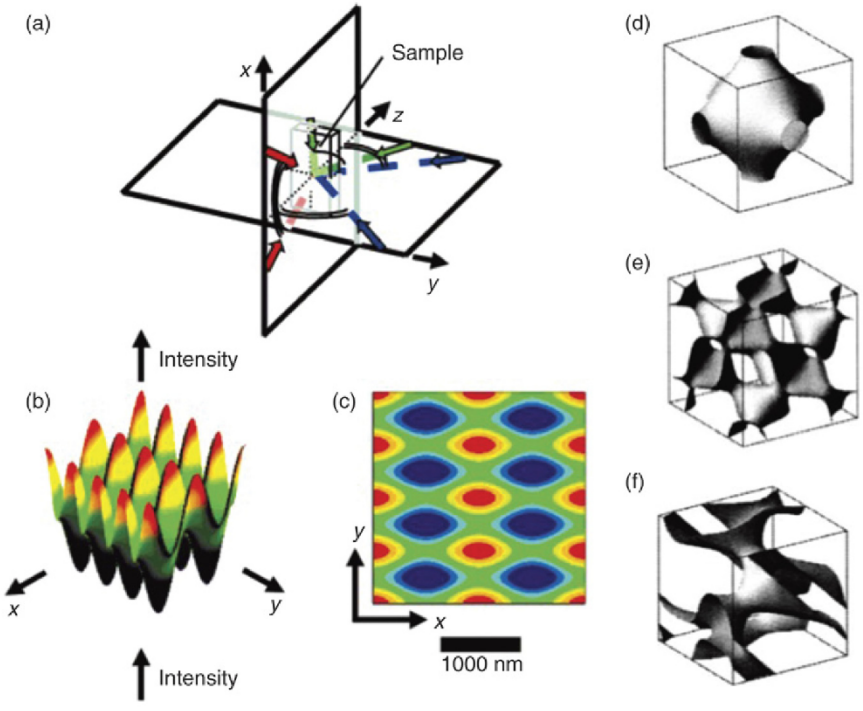

FIGURE 6.7 **Interference stereolithography relies on creating interference patterns between multiple coherent light waves in order to create patterns of high and low intensity light fringes.** (a) Beam and sample geometry for creating interference pattern. Arrows of the same color represent coherent beams and arrows of different colors represent mutually incoherent (i.e., orthogonally polarized) beams; (b) intensity pattern generated by laser beam interference; (c) color map of intensity pattern projected onto the *x*–*y* plane; (d) simple cubic P structure intensity map for interference stereolithographic fabrication; (e) diamond-like structure with FCC translational symmetry for interference stereolithographic fabrication; (f) gyroid-like structure with BCC translational symmetry for interference stereolithographic fabrication. (Figure 6.7a–c reprinted with permission from Tondiglia et al. [14]; Figure 6.7d–f reprinted with permission from Ullal et al. [16]).

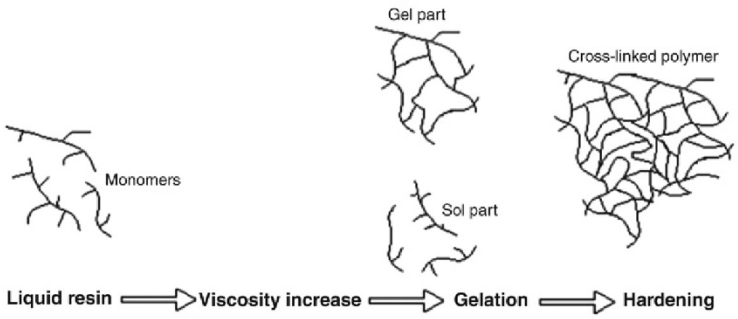

FIGURE 6.8 Schematic of cure mechanism of polymerizable oligomer. Resin is composed of liquid photosensitive resin that forms reactive radical species when irradiated with light. These radicals begin to propagate via cross-linking to form gel-like networks. Following termination of the polymerization process, a solid cross-linked network is formed [5].

to form cross-linked networks. The formation of covalent bonds in these networks *terminates* the polymerization process (Fig. 6.8).

Radical photoinitiators are a crucial component of stereolithographic resins. They belong to a family of reactive chemical compounds that decompose to form high-energy free radicals, or molecules with unpaired valence electrons, when exposed to light. In single-photon stereolithography processes, a single photon from the irradiating light source is sufficient to excite the photoinitiator into this high-energy state. In multiphoton stereolithography processes, the simultaneous or sequential absorption of two relatively low-intensity photons is required to excite a photosensitive resin to a high-energy radical state. In both types of processes, photoinitiators help to initiate the stereolithographic polymerization process by forming the reactive radical species that drive polymerization of oligomers in the resin material. The choice of photoinitiator determines the rate of polymerization, or curing, of the resin. As several photoinitiators are cytotoxic, the family of photoinitiators suitable for applications in biomedical engineering is limited, as discussed in Section 2.2.1.

The primary component of a stereolithographic resin is the polymerizable oligomer. Following the initiation of the polymerization process by radical photoinitiators, the functional groups of polymerizable oligomers form active radicals that react with one another to form cross-linked polymerized networks. Conventional SLA processes rely heavily upon fabrication with acrylate and methacrylate oligomers, epoxide, and vinyl ether-based resins that cure rapidly upon irradiation and whose chemical formulas can readily be modified to obtain materials with a variety of geometric and material properties. Indeed, many polymerizable oligomer systems currently used for stereolithographic biofabrication applications rely on biocompatible oligomers containing acrylate and methacrylate functional groups that form radicals in response to photoexcitation. A detailed description of the composition and material properties of the most commonly used stereolithographic resins for biomedical applications is presented in Section 2.2.2.

The process of curing photopolymerizable resins via conventional stereolithography is very well understood and is easily characterized via an adapted form of the Beer–Lambert equation, which is a relationship between the intensity of a light source and the exponential decay it experiences as it passes through an absorbing medium. This adapted equation, termed the cure-depth equation (Eq. 6.1), demonstrates the relationship between the amount of UV radiation that a liquid resin is exposed to and the depth to which the resin is cured as an effect of radiation penetration:

$$C_d = D_p \ln\left[\frac{E_{max}}{E_c}\right] \tag{6.1}$$

Where C_d represents the maximum cure depth of the resin, D_p represents the penetration depth at which UV energy intensity is reduced to $1/e$ of its maximum value at the surface of the resin (e is the mathematical constant that forms the base of the natural logarithm), E_{max} is the maximum UV energy intensity at the resin surface, and E_c is the critical energy intensity required to cure the resin by triggering its transition into a solid phase.

Resins are generally characterized by their penetration depths and critical energy. The penetration depth corresponds to the extinction coefficient, or molar absorptivity, of the irradiated resin. This characteristic value can be tuned and modified by adjusting the concentration of photoinitiator solution present in the resin. It can also be modulated by the addition of visible-light or UV-absorbing dyes, which compete for irradiation absorption during the polymerization process [17]. Values of D_p are tuned to prevent "over-cure," or excessive exposure to UV light caused by repeated irradiation during the layer-by-layer manufacturing process. Prevention of over-cure is of essential importance in preserving viability of cells in stereolithographic bioprinting applications targeting tissue engineering, as excessive UV exposure has a detrimental effect on cellular viability (see Section 4). The value of the critical energy for a resin, E_c, is likewise dependent on the concentration of photoinitiator present in the solution, as well as other dissolved gases (e.g., oxygen) or liquids (e.g., colored dyes) that could

compete for the absorbed light energy. The energy dose of the irradiating light source at the surface of the resin, corresponding to E_{max}, is regulated by modulating the scanning speed (for laser-based systems) or specifying the exposure time (for projection mask-based systems).

Precise calibration and modulation of the light energy dose and composition of the photosensitive resin therefore provides a simple and reliable method of controlling the cure depth. Plots of cure depth vs. energy dose for a given combination of stereolithographic apparatus and resin are termed "working curves." These working curves are used to select the conditions that provide cure depths that ensure adhesion to the fabrication support platform as well as to adjacent layers of the 3D fabricated part. Reduced cure depths provide more accurate control of thickness and provide higher quality finishes to manufactured parts. However, decreased cure depths correspond to increase number of layers and hence increased build-time.

For applications in conventional manufacturing sectors, parts manufactured via stereolithography are often subjected to a postcuring process, which involves uniform exposure to UV irradiation that helps improve the mechanical properties of the fabricated parts. This step is often not required for translational biomedical applications, as many such applications do not require extremely high mechanical strengths, but various postfabrication steps used to clean and sterilize fabricated parts have been employed, as discussed later in this chapter.

2.2.1 Radical Photoinitiators for Stereolithographic Biofabrication

Different photoinitiators are distinguished by the wavelength range in which they present high-energy absorption, and are thus readily described by their unique absorption spectra. The choice of excitation light source wavelength and photoinitiator composition are thus inextricably linked to one another. A general trend in excitation wavelength is that the shorter the wavelength of UV light, the better the resolution of fabricated feature sizes. However, this decrease in excitation wavelength is paired with lower penetration depth into the sample and hence increased build-time [18].

A variety of photoinitiators have been developed to suit a range of photopolymerization applications, but most photoinitiators are cytotoxic (i.e., cause cell death), which renders them inappropriate for use in biomedical applications. For such translational medical applications, the wavelength criterion poses a further challenge for adapting stereolithographic technology, as it is essential in such cases to limit the oxidative damage to biological components caused by exposure to high-energy irradiation. These stringent limitations severely constrain the size of the relevant family of photoinitiators that can be used in biomedical applications. However, by characterizing the cytotoxicity of relevant photoinitiators and incorporating postprocessing steps, such as repeated "washes" and sterilizations, researchers have succeeded in fabricating 3D structures that can safely integrate with biological tissues and organs. The success of finding a range of photoinitiators that match the design criteria required for biomedical applications has demonstrated feasibility of using stereolithography for a broad range of applications including patient-specific prosthetics, implants, and scaffolds for tissue engineering.

Tissue engineering applications pose the most stringent restrictions on the photoinitiator compositions that can be incorporated in stereolithographic resins, as they require living cells to come into direct and prolonged contact with these reactive compounds. Furthermore, the viability of living cells exposed to high-intensity irradiation is very sensitive to the wavelength of the light source – cells are more viable upon irradiation of wavelengths in the UV A (400–315 nm) range than in the UV B (315–280 nm) or UV C (280–100 nm) range. Thus, photoinitiators with absorption spectra in the UV A range are most suitable for applications involving resins containing living cells. It is to be noted that the absorption spectra of photoinitiators can be modified by adjusting the concentration of photoinitiator present in the photopolymer resin, as increasing the photoinitiator concentration ensures that irradiation from a broader range of target wavelengths can be utilized.

The most commonly used commercially available photoinitiator for applications in tissue engineering by conventional stereolithography is 2-hydroxy-1-[4-hydroxyethoxy) phenyl]-2-methyl-1-propanone, also known as Irgacure 2959. The cytotoxicity profile of this photoinitiator has been very well characterized by several studies. Elisseeff and coworkers published an extensive comparison of the cytotoxicity profile of Irgacure 2959 and other commonly used UV light sensitive photoinitiators on a broad range of mammalian cell types and species [19]. This study demonstrated minimal cytotoxicity of Irgacure 2959, as compared to other UV irradiation sensitive photoinitiators. Furthermore, this study demonstrated that resin cytotoxicity is highly sensitive to the concentration of photoinitiator, as expected, and that different cell types have varying degrees of sensitivity to identical concentrations of a given photoinitiator. The advantageous properties of Irgacure 2959 as demonstrated by this and other studies have, therefore, contributed to its popular use in conventional stereolithography-based systems to manufacture 3D structures with encapsulated cells (Fig. 6.9).

Advances in photoinitiator chemistry have been further driven by Anseth and coworkers, who have developed a photoinitiator, lithium phenyl-2,4,6-trimethylbenzoylphosphinate (LAP) that demonstrates increased sensitivity to UV light and is also sensitive to wavelengths in the visible light range [20]. By enabling the use of reduced photoinitiator concentrations and lowered light intensities, LAP has demonstrably superior capacity to preserve the viability of

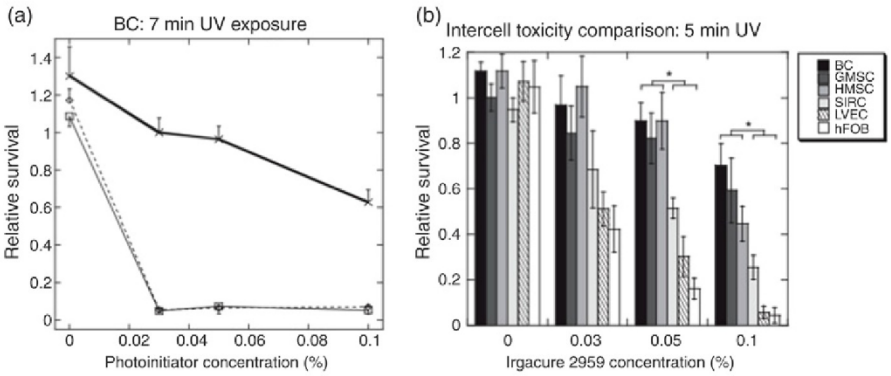

FIGURE 6.9 The relatively low cytotoxicity of Irgacure 2959, as compared to other commonly used photoinitiators, renders it favorable for use in encapsulating cells via stereolithography. (a) Relative survival of BC cell line after 7 min of UV exposure in resin containing Irgacure 2959, HPK, or Irgacure 651 photoinitiator; (b) relative survival of six cell types (BC, gMSC, hMSC, SIRC, LVEC, hFOB) after 5 min of UV exposure in resin containing variable concentrations of Irgacure 2959 [19].

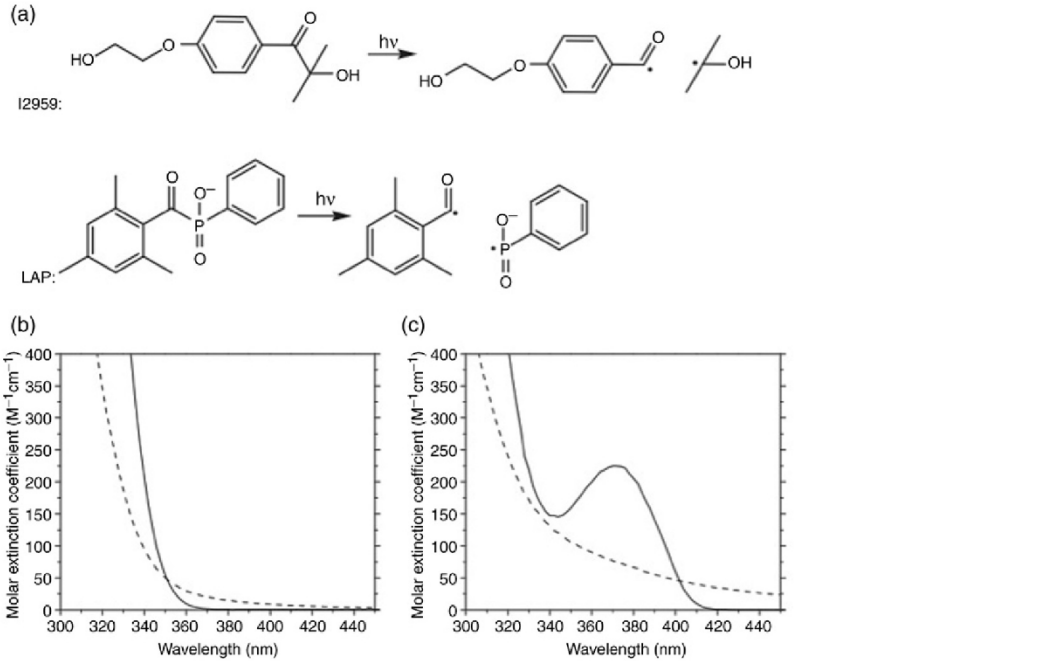

FIGURE 6.10 Irgacure 2959 and LAP are two of the most successfully used photoinitiators for biocompatible stereolithography with resins containing living cells. (a) Schematic showing photon absorption leading to cleavage of Irgacure 2959 and LAP into radical reactive species; (b) molar absorptivities of Irgacure 2959 (-) and cleavage products (--); (c) molar absorptivities of LAP (-) and cleavage products (--) [20].

cells encapsulated in stereolithographic resins. As this field continues to grow and applications of stereolithography in regenerative medicine become more popular, it is likely that further research will target the discovery of photoinitiator compounds with advantageous properties similar to or perhaps greater than those demonstrated by Irgacure 2959 and LAP (Fig. 6.10).

2.2.2 *Biocompatible Polymerizable Oligomers for Stereolithographic Biofabrication*

Stereolithography systems for conventional manufacturing applications have, as mentioned in an earlier section of this chapter, primarily used reactive acrylate/methacrylate, epoxide, or vinyl ether-based resins, or some hybrid composition thereof [5]. As stereolithographic fabrication technology expands to target translational medical applications, the number of suitable resins decreases slightly, but is not as restricting as the requirements posed on photoinitiators discussed in Section 2.2.1. This is because most cross-linked polymers are not toxic in themselves, though the unreacted monomers and residues of reactive photoinitiator residues may have cytotoxic effects. In many cases, post-processing steps such as washes with water and/or alcoholic solutions, sterilization with UV light irradiation, or

treatment with supercritical carbon dioxide (which introduces microporosity into fabricated structures in addition to removing toxic residues [21]) have proven sufficient to ensure biomedical applicability of a resin composition.

It is to be noted, however, that there are still many quality criteria that must be met in order for a stereolithographic resin to be considered suitable and desirable for biofabrication. Photosensitive resins for biomedical applications must, in addition to efficiently absorbing and curing in response to light irradiation, be biocompatible. That is, they must integrate with the target biological host without having a toxic effect on the living system. Biomedical applications also often require materials that are biodegradable (controllably disintegrate in response to host environmental cues leaving only nontoxic byproducts) and bioactive (actively promote beneficial and regenerative effects in the host biological system).

2.2.2.1 High-Strength Resins

For biomedical applications that require high mechanical strength, such as load-bearing implants, polymer-ceramic composite materials combine strong mechanical properties with demonstrable biocompatibility [22]. Formulation of these ceramic-based resin materials is primarily accomplished by mixing ceramic particles, most often alumina or hydroxyapatite, with a liquid photopolymer [23–25]. It is to be noted that such powder-infused resin compositions are often extremely viscous, and must hence be mixed with diluents as described previously. Furthermore, the ceramic particles in these resins must be significantly smaller than the resolved feature sizes and layer thickness within the fabricated part in order to maintain fabrication quality/accuracy [26].

2.2.2.2 Elastomeric Resins

An important constraint on relevant stereolithographic resins is posed by the mechanical properties that are required of biomedical devices. Most conventional SLA resins are glass-like/brittle because they are composed primarily of low molecular weight monomers that react to form rigid cross-linked networks. By contrast, biomedical applications require materials that are more elastomeric (i.e., compliant/flexible) in nature. Resins formulated for these applications thus comprise high molecular weight macromers with relatively low glass transition temperatures. Since liquid suspensions of such macromers are often very viscous, fabrication with such resins often requires mixing with either nonreactive or reactive diluents, such as *N*-methylpyrrolidone, *N*-vinyl-2-pyrrolidone (NVP), diethyl fumarate (DEF), or water, to reduce resin viscosity and increase fabrication resolution and accuracy [1]. These diluents have demonstrably increased the hydrophilicity and biocompatibility of SLA-fabricated structures for a variety of resin compositions [27,28]. It is to be noted that nonreactive diluents, such as *N*-methylpyrrolidone, are more applicable when the macromer contains more reactive groups such as acrylates or methacrylates.

Historically, stereolithographic systems have made extensive use of (meth)acrylate-based and epoxy-based resins for fabrication. Epoxy-based resins are generally cytotoxic and hence unsuitable for translational medical applications. On the other hand, modified polyether (meth)acrylate-based systems, such as those developed by Emons and coworkers, have been proven to be biocompatible via *in vitro* tests on mouse fibroblasts [29]. Furthermore, these biocompatible resins form elastomeric polymers that are more flexible than conventional SLA-fabricated materials, displaying a broad range of tunable material properties (hardness, stiffness, etc.) that can be tailored to suit various biomedical applications (Fig. 6.11).

2.2.2.3 Biodegradable Resins

Often, *in vivo* applications of SLA fabricated biomedical devices require that the fabricated structures biodegrade in a precisely controlled and nontoxic manner, in order to encourage the regeneration of host tissue at the site of disease or trauma-induced damage. As a consequence, the field of research targeting formulations of biodegradable photosensitive resins has been very active in recent years.

Matsuda et al. initiated early developments in this field by developing a photosensitive biodegradable oligomer through ring-opening polyaddition of trimethylene carbonate (TMC) with ε-caprolactone [30,31]. Degradation behaviors of these polymers induced by hydrolytic surface erosion were measured *in vivo* via subcutaneous implantation of SLA-fabricated microstructures in rats [32]. Similar work on TMC-based biodegradable polymers by Cho and coworkers demonstrated the use of such materials to create scaffolds for regeneration of cartilage and bone [33].

In early demonstrations by Dean and coworkers, SLA systems were successfully used to manufacture biocompatible and biodegradable structures with poly(propylene fumarate) (PPF) based photosensitive resins mixed with DEF diluent [34]. Further characterization and *in vitro* testing of such PPF/DEF biodegradable systems have promising implications for a diverse array of tissue engineering applications [28,35,36].

Grijpma and coworkers have developed SLA-compatible poly(D,L-lactide) (PDLLA) biodegradable resins mixed with NVP diluent, creating hydrophilic polymerized networks with good cell-adhesive properties as demonstrated by *in vitro* tests with mouse preosteoblasts [27]. Further developments by this group eliminated the need for such reactive diluents, which are nonbiodegradable, by replacing them with the nonreactive diluent ethyl lactate and further improving the biodegradability of SLA-fabricated structures [37].

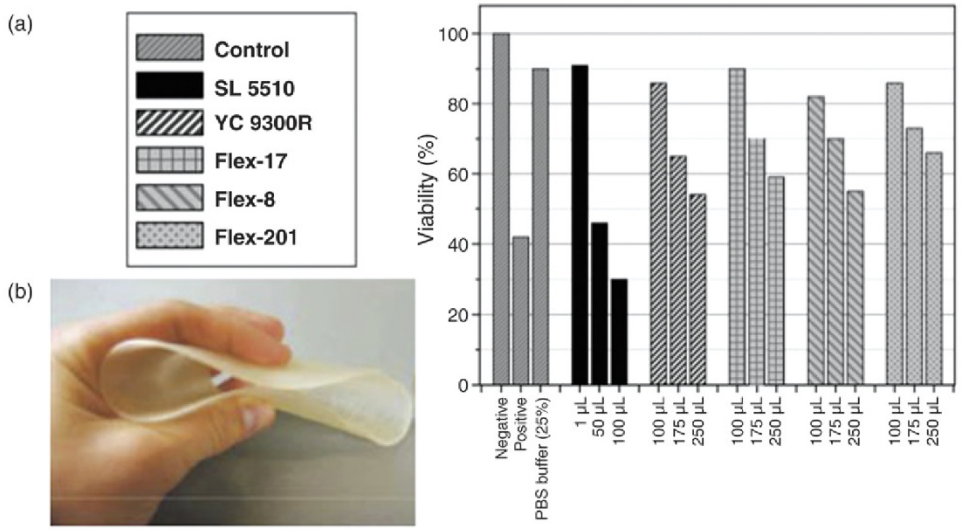

FIGURE 6.11 **Elastomeric resins for stereolithography that allow for the fabrication of compliant/flexible parts are of especial relevance in biomedical and translational applications.** (a) Cytocompatibility of elastomeric resins developed by Emons and coworkers. SL 5510 is an acrylate/epoxy-based formulation, YC 9300 R is an acrylate-based formulation, and the Flex materials are polyether(meth)-acrylate-based formulations; (b) a flexible breathing mask fabricated using the novel biocompatible Flex material [29].

2.2.2.4 Hydrogel Resins

The resins presented in this section have thus far been compatible for applications that involve fabrication of biomedical devices/structures that come into contact with biological systems after postprocessing steps. However, next-generation regenerative medicine applications that fall under the category of "tissue engineering" herald the need for stereolithographic resins that contain living cells. The most promising of photosensitive polymeric materials that support this requirement are a broad class of hydrophilic and biocompatible materials known as "hydrogels."

Cross-linked polymeric hydrogel networks are highly porous and absorbent, facilitating the diffusion of biochemical signals and essential nutrients through the polymeric network. Their structural and functional properties, such as network porosity and hydrophilic swelling behavior, can be readily tailored via chemical modifications to the monomers present in the resin. Their mechanical properties, which fall in the range of 1–100 kPa, are more suited to applications targeting engineering of soft tissues such as those present in the human body. Furthermore, hydrogels also have the ability to respond to changes in temperature, pH, illumination, or other physical and chemical stimuli. This is particularly advantageous for biomedical applications that rely on real-time response behavior such as dynamic medical implants or bioactuators that generate force in response to external stimuli. For these reasons, systems incorporating hydrogel polymers have seen widespread use in translational medical applications in recent years [38,39].

In a pioneering study in this field, Boland and coworkers presented the first demonstration of encapsulating live cells within a photopolymerizable hydrogel via stereolithography. A hydrogel prepolymer solution comprising a mixture of poly(ethylene oxide) and poly(ethylene glycol) dimethacrylate (PEGDMA), reminiscent of the (meth)acrylate-based polymer chemistry discussed earlier in this chapter, was mixed with Irgacure 2959 photoinitiator and Chinese hamster ovary (CHO) cells and polymerized using a direct-laser writing single-photon stereolithography machine [40]. Viability of cells cultured *in vitro* within these polymerized hydrogel constructs was assessed via live/dead assay, proving that SLA-based technologies could be used to fabricate high-density elastomeric tissue-like constructs.

Wicker and coworkers expanded upon this early work, which demonstrated fabrication of relatively simple geometry constructs, to viably encapsulate living cells in PEGDMA hydrogels with more complex 3D geometries via SLA [41]. The hydrogel prepolymer formulation in this case used a combination of two photoinitiators, Irgacure 2959 and 2-hydroxy-2-methyl-1-phenyl-1-propanone. The soluble fraction and swelling ratios of fabricated hydrogels were characterized, providing an understanding of the underlying mechanisms that govern the geometric properties of fabricated parts as a result of polymer resin chemistry (Fig. 6.12).

2.2.2.5 Bioactive Resins

These and other early studies with PEG-based hydrogels, while promising, were still limited by the fact that cells do not naturally form strong adhesive interactions with networks of synthetic polymers. To target this, the study by Wicker and coworkers explored the effect of covalently incorporating the cell-adhesive ligand RGDS (Arg–Gly–Asp–Ser tetrapeptide) within the fabricated hydrogel matrix

(a)

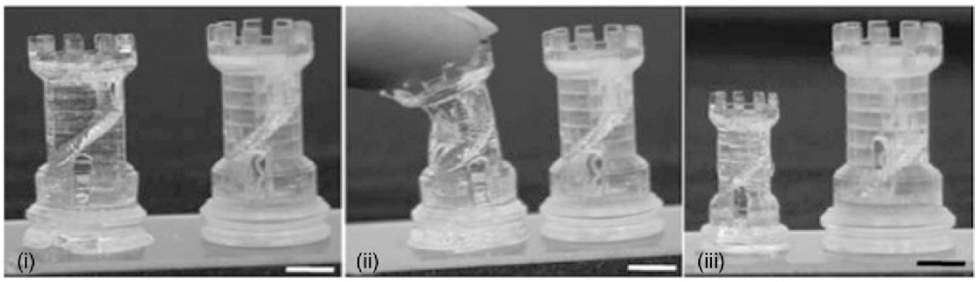

(b)

Well	Initiator concentration (μL)	Live cells (%)	Total no. of live cells
1	0	91.58	$8.62 \times 10^4 \pm 2.23 \times 10^4$
2	50	64.54	$6.07 \times 10^4 \pm 5.11 \times 10^4$
3	100	50.26	$4.74 \times 10^4 \pm 2.47 \times 10^4$
4	150	28.32	$2.67 \times 10^4 \pm 1.82 \times 10^4$
5	200	41.71	$3.93 \times 10^4 \pm 3.17 \times 10^4$
6	250	11.22	$1.06 \times 10^4 \pm 0 \times 10^4$

FIGURE 6.12 **The porous and absorbent nature of polymeric hydrogel resins make them the ideal biocompatible resin for stereolithographic fabrication with living cells.** (a) A complex 3D design of a chess rook immediately after fabrication: (i) following deformation via mechanical compression, (ii) and after drying, (iii) (scale bar 5 mm) [41]; (b) relative viability of CHO cells encapsulated in elastic hydrogel matrices via stereolithography. Increasing photoinitiator concentration leads to decreased viability [40].

to provide cell-adhesive attachment sites throughout the polymerized structure. Bashir and coworkers expanded upon this work by assessing the effect of RGDS on the long-term viability of cells encapsulated within PEG-based hydrogels of varying molecular weights [42]. Addition of these adhesive peptide sequences showed significant increases in cell viability, proliferation, and spreading as compared to control samples, demonstrating that the incorporation of bioactive moieties within polymeric networks could remove this limitation from SLA-fabricated hydrogel structures. West and coworkers expanded this work by using two-photon laser scanning photolithography to precisely dictate the placement of RGDS peptides within 3D fabricated acrylate-modified PEG hydrogel architectures [43] (Fig. 6.13).

Others have similarly investigated the effects of incorporating different types of bioactive compounds within polymeric matrices. Farsari et al. utilized a multiphoton photopolymerization apparatus to immobilize biotin linked to fluorescently labeled streptavidin to 3D fabricated structures, demonstrating the ability to bind proteins to structures via SLA [11]. Similar work by Woodbury and coworkers utilizing a scanning laser-based SLA in conjunction with methacrylate-based polymer resins to selectively graft peptides onto 3D fabricated microstructures and study postsource decay sequencing of peptides [44]. Bashir and coworkers have demonstrated spatially selective and controllable patterning of proteins on hydrogel polymers by combining a microcontact printing approach with a direct-laser writing SLA setup, showing that cell patterning and alignment in 3D structures can be readily controlled by such a process [45]. Roy and coworkers have also demonstrated the use of SLA to spatiotemporally pattern scaffolds with extracellular matrix components, such as heparan sulfate, and polymeric microparticles containing heparan-binding growth factors, such as basic fibroblast growth factor-2 [46]. By demonstrating controlled predesigned spatiotemporal distribution of multiple bioactive factors within SLA-fabricated polymeric matrices, these and other studies have set the stage for engineering complex tissue-engineered structures through multilineage differentiation of a single encapsulated population of stem cells.

An alternative approach to separately incorporating bioactive moieties into polymerized matrices is to modify the chemistry of oligomeric monomers used in photosensitive resins. Liska and coworkers used a stereolithographic process to polymerize various methacrylate-based gelatin derivatives, demonstrating the ability to fabricate arbitrary cellular structures with a range of cell types [47]. Other modified methacrylated PEG- and gelatin-based systems incorporating oligopeptides into hydrogel networks have shown that such polymeric scaffolds significantly enhance cell adhesion and growth as compared to nonmodified materials [48]. Chen and coworkers have made extensive use of similar gelatin methacrylate (GelMA) hydrogel materials as a photosensitive resin for high-resolution 3D patterning using a projection SLA, demonstrating the biological functionality of such manufactured constructs [49].

Methacrylate modification of naturally occurring polysaccharides, such as hyaluronic acid [50] and chitosan [51], has likewise been used in photosensitive resin compositions for applications in stereolithographic biofabrication targeting tissue repair and regeneration. Recent studies by Schober and coworkers have even demonstrated multiphoton laser-based photofabrication of unmodified native polymers, such as collagen and fibrinogen, and liquids, such as natural human blood and fetal calf serum [52].

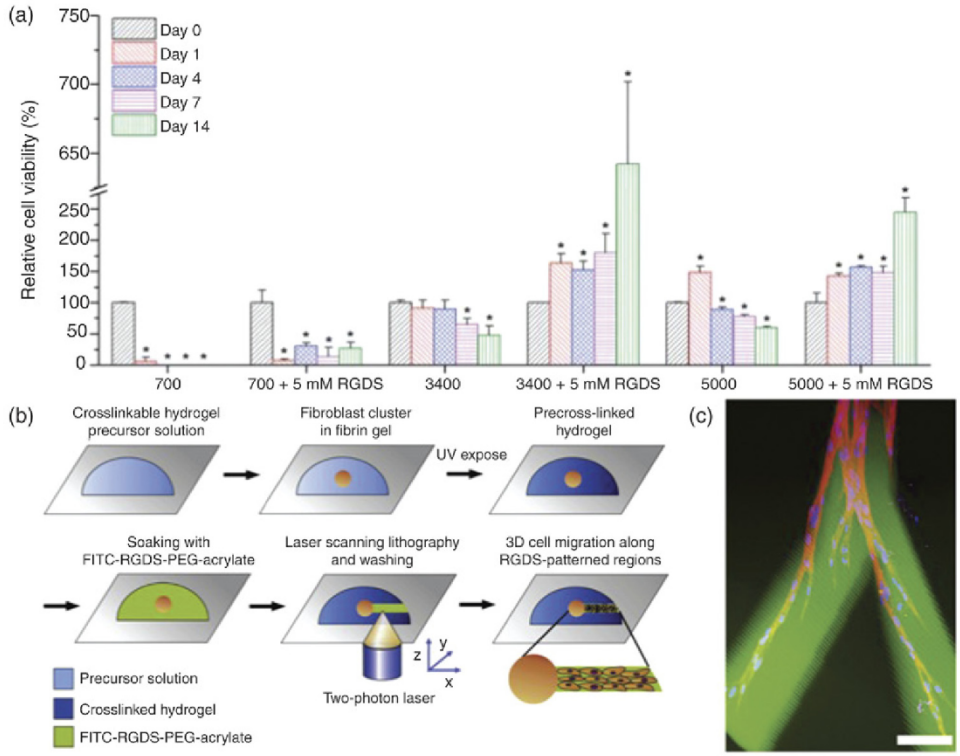

FIGURE 6.13 **Incorporating bioactive moieties, such as the cell-adhesive ligand RGDS, in stereolithographic resins can improve the viability and proliferation of cells encapsulated within the resins.** (a) Relative viability of cells encapsulated in PEG-based hydrogels of varying molecule molecular weight with/without incorporated RGDS ligands [42]; (b) selective patterning of RGDS peptides within 3D PEG-based hydrogels via two-photon stereolithography [43]; (c) confocal microscope image of human dermal fibroblasts cells (red and blue) undergoing migration within the RGDS-patterned region (green) of a PEG hydrogel (scale bar = 100 μm) [43].

2.2.3 *Multimaterial Stereolithographic Fabrication*

While all the polymers described in this section are useful for a variety of biomedical applications, true versatility of the stereolithographic process can only be attained by multimaterial fabrication of complex 3D structures. This type of multimaterial SLA fabrication can be accomplished by selectively polymerizing portions of layers with a single resin type, washing away unpolymerized resin, and then adding and polymerizing a different resin, as demonstrated by Wicker and coworkers [8]. Bashir and coworkers incorporated a similar multistep system to fabricate 3D cell-encapsulating multimaterial hydrogel structures using a laser-based apparatus [42]. This set the stage for using multimaterial SLA processes to coculture systems of cells, such as neurons and skeletal muscle, to study intercellular interactions and establish a basis for engineering complex tissues and organs containing multiple encapsulated cell types [53] (Figs 6.14 and 6.15).

2.2.4 *Novel Resin Systems*

As stereolithography has grown to become a fairly well established commercial process, the number of photosensitive resins that rapidly solidify in response to light-excitation has correspondingly increased. The morphological, mechanical, and material properties of these polymerizable resins cover a broad range and are broadly relevant for a variety of translational applications in the field of biomedical engineering. However, the number of photopolymerizable resins for stereolithography that are compatible with applications in bionanotechnology are still limited. A few of the most commonly used families of resins in this field have been elaborated upon in this section, and detailed information regarding photosensitive noncytotoxic resins are listed in more extensive reviews [54,55], but the rapidly changing nature of this field ensures that the variety of available resins will continue to increase and diversify in the coming years.

2.3 Applications of Stereolithography in Biomedical Engineering

The vast array of biomedical and translational applications of stereolithographic fabrication fall into a series of broad categories: Manufacturing of (1) data visualization and surgical planning tools to aid clinicians; (2) individualized prosthetics; (3) customized implants and surgical tools;

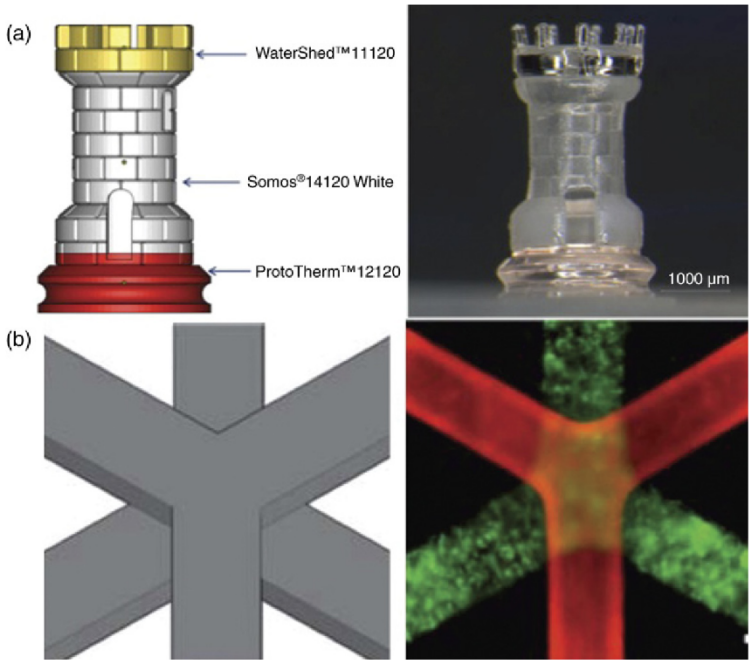

FIGURE 6.14 Multimaterial stereolithography enables the fabrication of complex 3D structures with varying mechanical, material, and functional properties. (a) Chess rook design fabricated using three different photosensitive resins [8]; (b) NIH/3T3 cells tagged with either green or red dye encapsulated in different distinct layers using stereolithography, showing viability of multimaterial approach for resins containing living cells [42].

(4) biomaterial scaffolds for tissue engineering; (5) high-density cellular constructs for tissue engineering. These applications are further elaborated upon in Sections 3 and 4.

3 APPLICATIONS OF STEREOLITHOGRAPHY IN SURGICAL PROCEDURES, PROSTHESES, AND IMPLANTS

The vast majority of currently used pre- and postoperative surgical procedures, prostheses, and implants could benefit greatly from the integration of patient-specific models and customized design parameters. While this individualized treatment model would be infeasible using standardized manufacturing techniques, the relative ease of generating accurate digital models and rapidly fabricating prototypes via medical imaging and stereolithography renders patient-specific treatment feasible. Use of stereolithographic manufacturing to manufacture preoperative planning models, external prosthetics, implantable devices, and surgical guides and tools are discussed in this section.

3.1 Stereolithographic Fabrication of Preoperative Visualization and Planning Tools to Aid Clinicians

Structural models and analysis have been extensively used in the fields of architecture and civil engineering for decades, motivating the complex analysis of clinically relevant 3D models via a similar approach. Advances in clinical imaging of 3D structures via CT and MRI have greatly advanced the practicing clinician's ability to easily visualize exterior surfaces and some internal structures. Manufacturing of patient-specific models and three-dimensional representations of clinical data via stereolithography promises to carry these advances further by building physical representations of a patient's anatomy. These models can be tuned to represent both hard and soft tissues and colored to distinguish different internal structures or pathologies, such as tumors, thereby augmenting the complexity of patient-specific models and predicting/controlling the effectiveness and aesthetic result of surgery [56]. Tools and models manufactured via stereolithography promise to aid clinicians in gaining a complex spatial understanding of patient anatomy, studying pathologies, making accurate diagnoses, and preoperative planning.

3.1.1 Patient-Specific Models

Stoker and coworkers demonstrated early efforts in the construction of patient-specific anatomical models by using an SLA to manufacture plastic models of the internal anatomy within a closed skull, as imaged by CT [57]. Providing a 3D physical representation of the internal anatomy of the skull has obvious applications in both physician and patient education, and can further aid as a model for surgical planning. Further developments in this field by

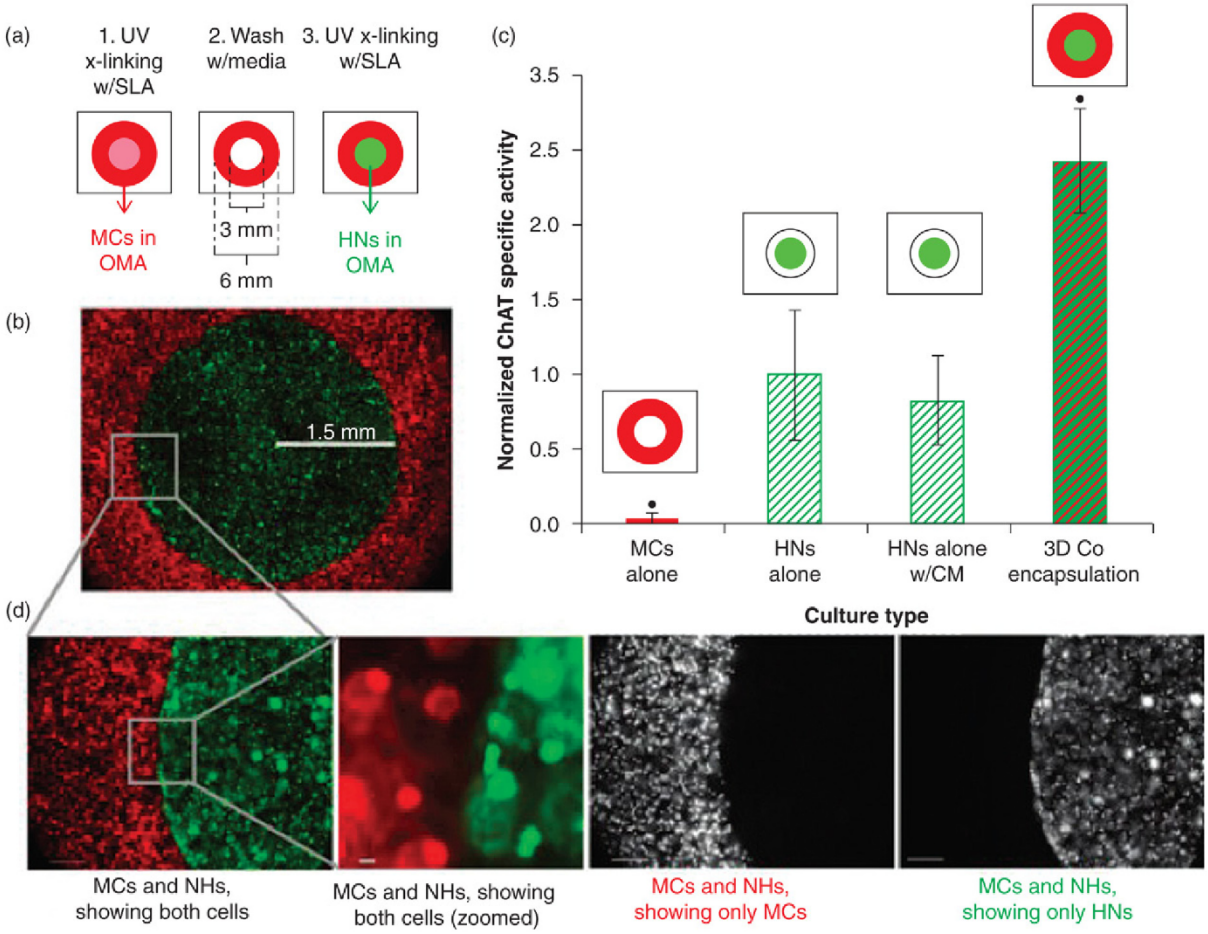

FIGURE 6.15 Multimaterial stereolithography can enable fabrication of 3D cell coculture systems to study intercellular interactions and establish a basis for engineering complex and functional 3D tissues. (a) Schematic of stereolithographic fabrication of resin containing either hippocampus neurons or skeletal muscle myoblast cells; (b) neurons and myoblasts encapsulated within single 3D structure via stereolithography; (c) bar graph showing increase in choline acetyltransferase specific activity for cells encapsulated in 3D multimaterial coculture system; (d) magnified fluorescence images of patterned multimaterial structure [53].

Wittenberg and coworkers demonstrated the use of stereolithography in maxillofacial operation planning by checking the "fit" of a human donor source for cranioplasty prior to surgical intervention [58]. This surgical planning step enabled by stereolithography was shown to demonstrable reduce operative risks and treatment time and improved postoperative results.

3.1.2 *Preoperative Planning Tools*

More recently, the efficacy of using CT/SLA-fabricated templates for oral implant surgeries have shown that such preoperative planning tools have a higher likelihood of implant survival and significantly lower deviation from planned implant positions [59]. Indeed, studies have shown that such stereolithographic surgical templates, in addition to allowing precise translation of surgical treatment plans into practice, also offer significant benefits over traditional procedures in more complex cases [59].

Implants that must function in high load-bearing environments, such as total hip replacements, require even more careful preoperative planning to ensure proper surgical placement. De Momi et al. utilized an SLA-fabricated preoperative planning model to visualize the physiological movement of the hip joint during daily life activities and generate data on patient gait analysis [60]. Understanding the load-bearing capacity of this implant in the context of the specific patient model provided surgeons with an accurate guided approach to performing the actual implantation procedure (Fig. 6.16).

3.1.3 *Data Visualization*

Stereolithography has also found use as an aid to generate physical representations of clinical data that help clinicians visualize patient-specific scenarios. Maurer and coworkers introduced this concept by manufacturing polyacrylic hard copies of echocardiographic patient data in order to enhance

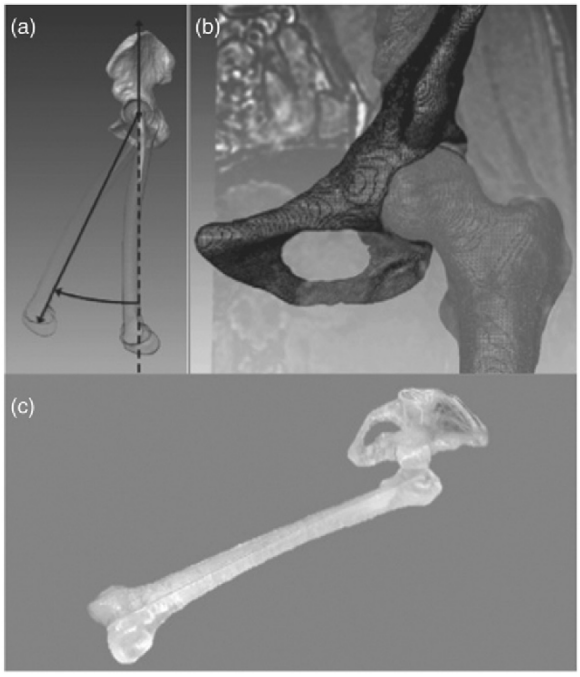

FIGURE 6.16 Preoperative planning tools manufactured via stereolithography can provide surgeons with a guided approach to performing complex surgical procedures. (a) Simulations used to perform patient gait analysis; (b) combined MRI and CAD modeling to produce model of required implant; (c) stereolithographic reconstruction of patient-specific model that can be used by surgeons for practicing placement in preoperative planning [60].

surgeon's spatial perception of the anatomy and pathology of the heart [61]. By providing anatomically correct models of mitral valve anatomy and pathology in patients, this 3D representation of data acquired via echocardiography helped improve the efficiency of diagnoses as well as preoperative planning for treatment of cardiovascular pathologies.

These and other studies first introduced stereolithographic fabrication into the field of medicine, by providing a customizable planning and educational tool for clinicians as well as patients. SLA-fabricated physical models have been used to fabricate complex external and internal structures within the human body and three-dimensional representations of clinical data sets. By providing clinicians with test-platforms and patient-specific models for preoperative planning, stereolithography has the potential to greatly impact the efficiency and accuracy of the diagnosis and treatment of a diverse set of pathologies.

3.2 Stereolithographic Fabrication of Individualized Prosthetics

Building upon this early work using stereolithography to fabricate patient-specific models and guide surgical planning, researchers began to use SLA processes to generate anatomically accurate 3D models that could be used directly as prosthetics. These individualized stereolithographic prosthetics can be customized to target a range of external patient defects [62].

3.2.1 Cosmetic Prosthetics

Initial studies in this field demonstrated much success in using stereolithography to fabricate high-quality patient specific hearing aids, setting the stage for mass customization of prosthetic devices [63]. Wilkinson and coworkers carried these developments further by utilizing a stereolithographic fabrication process to manufacture a customized whole-ear prosthetic from a wax resin [64]. In this study, information gathered from a digitized magnetic resonance image of a patient's ear was used to create a mirror-image 3D model of the missing contralateral ear. The digitized data were then converted into a 3D mold with a cavity corresponding to the shape of the missing ear and fabricated from a photopolymerizable silicone resin via stereolithography. A wax resin was then injected into the silicone mold to generate a prosthetic ear of the precise dimensions and morphology corresponding to the patient. Other auricular prostheses and personalized maxillofacial prostheses manufactured via mirror-image conversion of digital models have seen similar success as applications of stereolithographic fabrication [65]. As SLA technology has continued to evolve and the number of available resins has increased, direct mold-less fabrication of customized prosthetic devices has also been enabled (Fig. 6.17).

3.2.2 Load-Bearing Prosthetics

The manufacturing of more complex prosthetics for functional and weight bearing limbs, as opposed to mainly cosmetic enhancements, has likewise been enabled by new developments in chemically modified SLA resins with strong mechanical properties (i.e., hardness, stiffness, corrosion resistance, etc.). Preliminary studies in this field have used SLA technologies to test preliminary fitting of external prosthetics on patient-specific "test sockets." These sockets serve the purpose of testing the weight-distribution of the prosthetic to ensure that soft tissue is compressed only in pressure-tolerant areas. Ensuring a good fit through such test socket procedures is essential to the successful integration of the prosthetic with the patient. Stereolithographic fabrication of test-sockets for high load-bearing structures, such as transtibial prosthetics, has been successfully demonstrated [66] (Fig. 6.18).

3.3 Stereolithographic Fabrication of Customized Implants and Surgical Guides

The advances in prosthetics enabled by stereolithography illustrated in the previous section lead naturally to

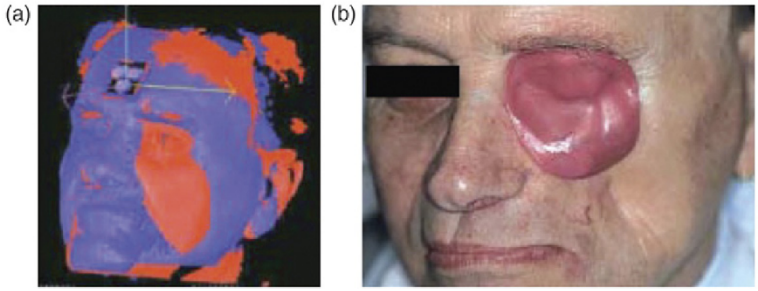

FIGURE 6.17 Cosmetic maxillofacial prosthetics manufactured via stereolithography can be readily customized and tailored to individual patients and different states of motion (e.g., mouth opening). (a) Digital scan and reconstruction of patient's face provides a model for rapid prototyping of cosmetic prosthetic; (b) prosthetic fabricated with the aid of stereolithography can be placed at the sight of damage and finished using conventional techniques [65].

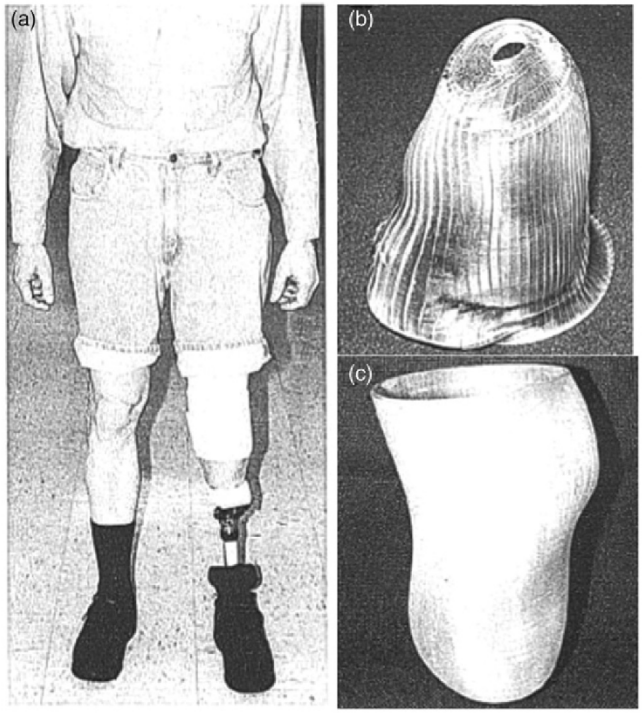

FIGURE 6.18 Manufacturing and testing test sockets for load-bearing prosthetics is critical to the long-term success of the prosthetic devices. (a) Transtibial amputee testing a socket fabricated via stereolithography for fit and functionality; (b, c) magnified view of two potential patient-specific test sockets for transtibial implant [66].

the use of stereolithography to manufacture customized patient-specific implants. These customized biocompatible implants, which must permanently integrate with a host biological system, promise to greatly improve the prospect for invasive surgical procedures targeting synthetic replacements of native tissue and organs.

Since implants, unlike external prosthetics, are in direct contact with native and regenerated tissue *in vivo*, it is critical to ensure the long-term biocompatibility of implant materials fabricated via stereolithography. A study by Popov et al. demonstrated that removal of potentially toxic residues of photosensitive resins (monomers, low molecular weight oligomers, etc.) could be accomplished via treatment with supercritical carbon dioxide, significantly enhancing the biocompatibility of the fabricated structures when implanted *in vivo* [21]. Other sterilization procedures using UV radiation or washes with alcoholic solutions have been similarly proven successful, as discussed further in Section 4.

3.3.1 Cosmetic Implants

Drawing upon the early advances in using stereolithography to fabricate external maxillofacial prosthetics, there have been many successful attempts to manufacture patient-specific implants for cranioplasty manufactured via stereolithography. Some approaches used CT data and SLA apparatus to design molds that were then used

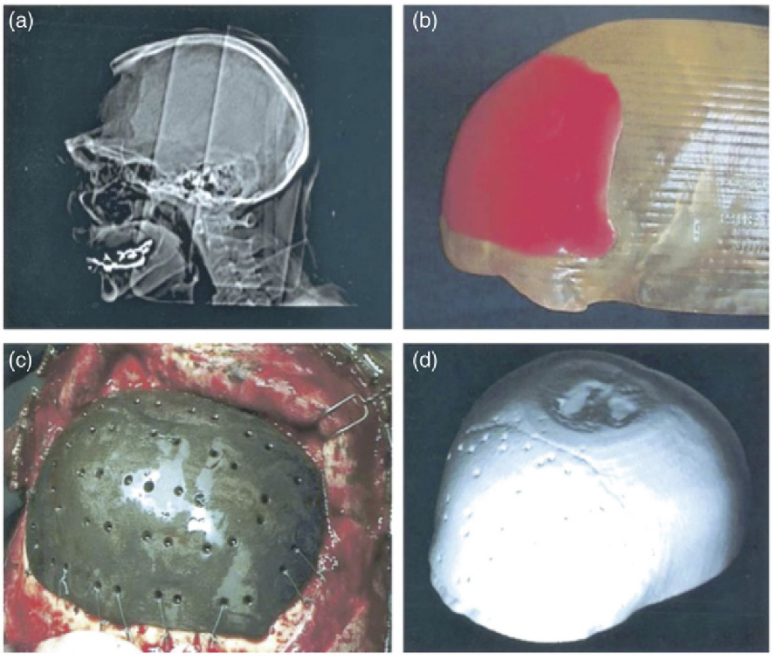

FIGURE 6.19 **Cosmetic maxillofacial prosthetics can be customized to patient-specific defects and readily fabricated via stereolithography.** (a) Digital scan of patient's large bifrontal defect; (b) model of patient skull fabricated via stereolithography and used as mold for implant generation; (c) patient-specific implant; (d) postoperative CT scan of implant showing excellent fit and integration with patient host [68].

to fabricate thermally polymerized custom implants from acrylic materials [67], or carbon-fiber reinforced polymeric composites [68]. More direct SLA-fabrication approaches have been demonstrated by Day and coworkers, who used a digital model obtained via contiguous helical CT scans to directly fabricate a patient-specific mandible via stereolithography to fit a large surgical defect obtained as a result of a tumor [69]. Fitting of the manufactured implant into the defect site provided aesthetically appealing results with good fit and integration of the fabricated mandible into the surrounding bone (Fig. 6.19).

3.3.2 Load-Bearing Implants

Customized design of load-bearing implants has been enabled by the creation of SLA-fabricated replica models of individualized patients. Early studies in this field aimed at individualizing total knee replacements for patients were shown to successfully return weight-bearing capacity to damaged limbs in both animal and human models [70,71]. Such customized implantation procedures have great value for all patient models, but especially in complicated cases where more individualized morphologies must be taken into account. As with the prosthetic devices mentioned earlier, further developments in creating SLA resins with strong mechanical properties (such as the polymer-ceramic composites detailed in Section 2) promise to result in the direct fabrication of patient-specific load-bearing implants.

3.3.3 Surgical Guides

SLA technologies have also been used to manufacture surgical guides that ensure proper placement of implants within patients. These guides are critical to the operative procedure, and are conventionally employed to direct implant drilling and placement systems. Customized surgical guides manufactured via SLA can greatly augment surgical outcome by improving the ultimate functional performance and design aesthetics of the implanted device. Rosenstiel and coworkers have demonstrated the reliability of surgical guides manufactured via stereolithography, showing that a significantly lower mean angular deviation was obtained for SLA surgically guided implants as compared to implants placed without SLA surgical guides [72]. These and other similar studies have demonstrated the ability to rapidly and accurately manufacture patient-specific surgical guides via stereolithography, thereby ensuring a high quality of pre-surgical planning and surgical execution on a customized case-by-case basis (Fig. 6.20).

4 APPLICATIONS OF STEREOLITHOGRAPHY IN TISSUE ENGINEERING AND REGENERATIVE MEDICINE

The field of tissue engineering is centered on the aim of creating complex biological substitutes for native tissue using a combination of cells and instructive biomaterials. This

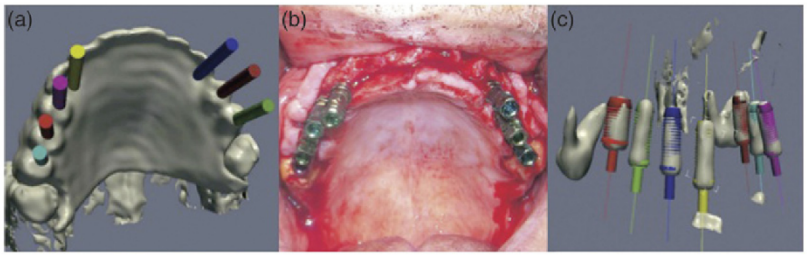

FIGURE 6.20 Patient-specific surgical guides fabricated via stereolithography can greatly improve the ultimate functional performance and design aesthetics of an implanted medical device. (a) CT scans and CAD modeling used to generate digital models of treatment planning guides; (b) implants placed using surgical guides fabricated via stereolithography; (c) demonstration of good match between planned implants (various colors) and actual placed implants (gray) [72].

emerging field promises to revolutionize modern medicine by providing an alternative to tissue and organ transplantation, and perhaps eliminating the need for implants and transplants altogether by aiding the rapid development and testing of new drugs and therapies [73]. The use of stereolithographic fabrication to fabricate biocompatible scaffolds for tissue engineering, followed by advances in this field pioneered by stereolithographic printing of living cells, is described in the following sections. As previously discussed in Section 2.2, advances in creating biocompatible, biodegradable, and bioactive photosensitive resins have enabled many of the advances in this field. These resins are tailored to prevent inflammatory response upon implantation, controllably degrade into nontoxic byproducts that can achieve good renal clearance, and actively encourage the formation of new regenerated tissue [74,75].

4.1 Stereolithographic Fabrication Strategies for Tissue Engineering and Regenerative Medicine

4.1.1 "Top–Down" Fabrication

The conventional approach to tissue engineering has been the fabrication of porous biocompatible and biodegradable scaffold structures as platforms for cell seeding. In the early stages of these studies, scaffolds were often generated using conventional microfabrication approaches for patterning natural and synthetic materials [76]. Researchers have even explored approaches in which cadaveric tissue is decellularized and repopulated with living cells to yield functional tissue and whole organs [77,78]. More recently, direct fabrication of biocompatible scaffolds via SLA processes has seen much success in a variety of tissue engineering applications (see Sections 4.2–4.5)

Scaffold-based approaches provide the ability to place cells within precise morphological designs while maintaining the cell–cell and cell–matrix interactions observed *in vivo*. However, these approaches come with the challenges of regulating the distribution of cells within the scaffolds, as well as the inability to engineer adequate vascular networks that can provide supplies of nutrients to large-scale engineered tissues. These challenges render scaffold-based "top–down" approaches undesirable for applications in tissue engineering of complex tissues and organs, as they are unable to provide truly precise spatial control of cells and biochemical signals in three dimensions [79].

4.1.2 "Bottom–Up" Fabrication

The rise of "bottom–up" approaches in biofabrication, triggered by the advent of highly absorbent biocompatible stereolithographic resins, provides and attractive alternative approach to manufacturing complex biological substitutes for native tissue and organs. In this approach, engineered tissues can be directly assembled layer by layer from the bottom up by using SLA resins containing encapsulated cells, allowing for complex three-dimensional control over the morphological and functional properties of engineered tissue.

The single-photon and multiphoton stereolithographic systems presented earlier in this chapter are ideal candidates for targeting applications in bottom–up tissue engineering. These systems have demonstrable high-resolution patterning capabilities and have been proven to viably encapsulate cells in polymeric networks while preserving viability and functionality in long-term studies by minimizing heat production and damage to raw material during fabrication.

4.1.3 Macro- and Microscale Architecture

High-resolution fabrication of three-dimensional porous structures with intricate internal geometries is a necessary requirement of top–down and bottom–up methods of manufacturing viable tissue-engineered constructs. Recent studies on the effect of microscale porous internal architectures of scaffolds on the repair and regeneration rate of damaged tissue have demonstrated the need for creating 3D structures with controllable morphologies on the macro- and microscales. This level of microenvironmental control has the further advantage of facilitating architecture for vascular networks and conduits, setting the stage for developing large-scale engineered tissues and organs in the future. High-resolution spatiotemporal patterning of bioactive moieties can also drive advances in multilineage differentiation

of a single population of encapsulated patient stem cells, creating truly customized replacement tissues. Hence, while many of the pioneering studies in SLA-based tissue engineering utilized the direct laser writing strategies and conventional UV irradiation driven polymerization, the rise of digital mask projection micro-SLA promise to further improve our ability to fabricate biodegradable and biocompatible architectures with single micron resolution [36]. Two-photon methods improve upon this even more by establishing biocompatible fabrication mechanisms with submicron resolution [12]. The fundamental challenge underlying all these fabrication strategies is based on negotiating the balance between fabricating macroscale structures while incorporating microscale features.

The use of SLA fabrication strategies to target regenerative medicine applications in tissue-engineered bone, cartilage, and cardiovascular tissue/networks are presented in the following sections. SLA technologies that target a range of other tissue/organ systems, such as liver, connective tissues, and neural conduits, have also been demonstrated, proving the readily customizable nature of this fabrication process.

4.2 Stereolithographic Fabrication for Bone Tissue Engineering

Tissue-engineered substitutes for bone are motivated by clinical need: skeletal defects, caused by disease or traumatic fracture, are increasingly common in a growing and ageing population and require treatment with bone grafts in order to retain functional output of the skeletal system [80]. Traditionally, autografts and allografts have been used to replace damaged tissue. However, these approaches come with the limitations of available supply, as well as an inability to directly match the patient-specific morphological and functional design requirements of the replacement bone to the native tissue that surrounds it [81].

4.2.1 Biocompatible Materials for Bone Tissue Engineering

Synthetic alternatives to bone grafts fabricated by traditional and SLA-based processes have been proven to have biocompatible material properties that render them useful in implant applications. Inspired by this early work in ceramic implants, Chu et al. demonstrated the use of a SLA to polymerize UV-curable polymer-ceramic composite scaffolds that were biocompatible and suitable for use as cell-seeding platforms [25]. These hydroxyapatite implants were implanted *in vivo* in Yucatan minipig models and shown to support the regeneration of bone tissue, as dictated by the internal architecture of the engineered scaffold. Similarly, work with vinyl ester resin based bone regeneration scaffolds fabricated via SLA and implanted *in vivo* in a rabbit model have shown active bone ingrowth and regeneration into the defect site [17] (Fig. 6.21).

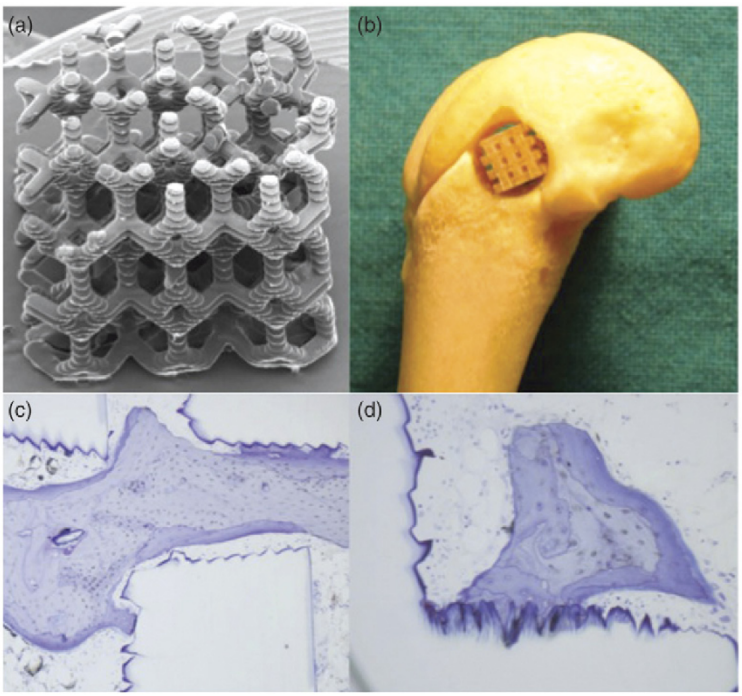

FIGURE 6.21 **Biocompatible scaffolds for bone tissue engineering manufactured via stereolithography.** (a) SEM image of SLA-fabricated scaffold manufactured with a biocompatible vinyl ester resin; (b) placement of SLA-fabricated scaffold *in situ*; (c) magnified view of fabricated scaffold 8 weeks after *in vivo* implantation showing newly formed bone with excellent host system integration; (d) bone apposition along serrated surface shows enhanced proliferation and growth in response to microscale scaffold architecture [82].

4.2.2 Biodegradable Materials for Bone Tissue Engineering

Synthetic structural materials often exhibit poor integration with the surrounding tissue; however, as a result of the mismatch between their morphological and mechanical properties and those of surrounding bone. Furthermore, as they are not bioresorbable, they do not represent a truly biointegrated solution to the skeletal defect. As a result, the field of regenerative bone engineering can only be advanced by developing complex 3D substitutes for bone tissue that can mimic the load-bearing mechanical properties and the morphological architecture observed *in vivo*, while allowing for biodegradation and active biointegration with the host/patient over time. Stereolithography is ideally suited to the task of creating such complex three-dimensional biodegradable substitutes for damaged bone tissue, and studies that make use of this technology have demonstrated significant advances in this field.

Early work in SLA fabrication using biodegradable resins for bone regeneration made extensive use of PPF resins diluted with DEF, as previously described in Section 2. Complex 3D scaffolds with intricate internal architectures were fabricated using this resin, with promising implications for bone ingrowth in implantation applications [28,34].

Grijpma and coworkers furthered this field by using stereolithography to manufacture scaffolds for bone tissue engineering using a novel PDLLA resin [37]. While other biodegradable macromers used in stereolithographic fabrication of bone tissue engineering scaffolds, such as TCM or PPF require mixing with a reactive diluent such as DEF to obtain appropriate viscosity [28], PDLLA is not so restricted. This ensured that a greater percentage of the final fabricated scaffold would biodegrade and resorb into engineered bone upon implantation of the scaffold into the biological system, promoting better biointegration with the host/patient. Furthermore, PDLLA was proven to be much stiffer than its polymeric counterparts, demonstrating an elastic modulus (a measure of material stiffness) of 3 GPa, which approaches the properties of bone tissue *in vivo* (3–30 GPa). Attachment and proliferation of mouse preosteoblasts cultured at physiologic conditions within these scaffolds demonstrated the viability of this approach for translational applications in bone tissue engineering (Fig. 6.22).

SLA-fabricated bone regeneration scaffolds have also been fabricated by chemically modifying natural polymers, such as the biocompatible and biodegradable polysaccharide chitosan. Wen and coworkers have shown that subcutaneous *in vivo* implantation of these natural material-based scaffolds in a rat model supported osteoconductivity and regeneration [51].

4.2.3 Microscale Architecture in Bone Tissue Engineering

Digital mask-based photolithographic methods have further improved on the precise fabrication of spatially patterned

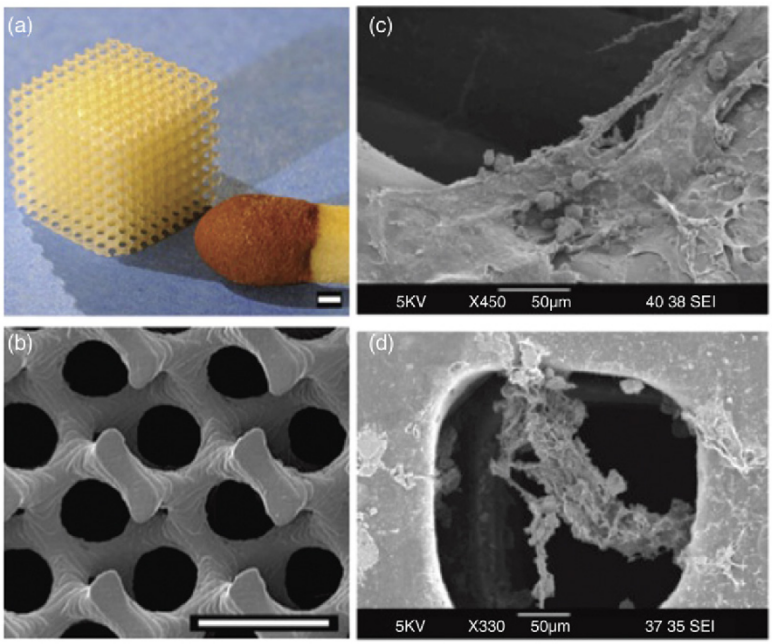

FIGURE 6.22 Biodegradable scaffolds for bone tissue engineering support the ingrowth and regeneration of bone. (a) SLA-fabricated scaffold manufactured using biodegradable resin; (b) SEM image of fabricated structure showing complex gyroid architecture; (c) 3D cell culture in SLA-fabricated scaffold showing cell adhesion, proliferation, and spreading on the scaffold surface 1 week postseeding; (d) cell migration and invasion in 3D into internal pores 4 weeks postseeding. *(Figure 6.22a,b reprinted with permission from Melchels et al. [37]; Figure 6.22c,d reprinted with permission from Lee et al. [35].)*

scaffolds for bone tissue engineering. Roy and coworkers have recently employed a DMD-based projection SLA to precisely distribute bioactive factors within a three-dimensional poly(ethylene glycol) diacrylate (PEGDA) scaffold with complex internal architecture [83]. The advantageous functional properties of these bioactive scaffolds were proven to drive osteogenic differentiation of marrow-derived stem cells *in vitro*, as indicated by postseeding mineralization of engineered tissue constructs.

Two-photon laser-based polymerization has also been used to target applications in bone tissue engineering by Ovsianikov et al. [84]. The photosensitive resin used in this study was a methacrylamide-modified gelatin derived from native collagen, and demonstrated chemical properties that mimicked the cellular microenvironment *in vivo*. The biodegradation properties of this material in response to collagenase digestion were quantified and proven to be tunable – a desirable property for any tissue engineered scaffold. Porcine mesenchymal stem cells seeded within these scaffolds demonstrated improved adhesion and proliferation behaviors. Osteogenic stimulants in the culture medium drove differentiation of these stem cells into the osteogenic line, with osteogenic cell byproduct calcium phosphate deposition observed in the scaffold.

4.2.4 Multifunctional Components for Bone Tissue Engineering

In addition to applications that target recreating the structure of cancellous and cortical bone, researchers have used stereolithography to fabricate the connective tissues found in bone marrow. Roy and coworkers used a DMD-based projection stereolithography system to manufacture scaffolds with intricate pore geometries, such as 3D honeycomb-like structures of interconnecting hexagons [7,83]. These 3D printed scaffolds then underwent surface modification to be functionalized with the ECM protein, fibronectin, and were sterilized prior to seeding with D1 cells, a murine bone marrow progenitor cell line. Successful seeding, attachment, and proliferation of D1 cells within these scaffolds was observed and quantified.

SLA-based fabrication technologies have, therefore, had significant impact on the bone regeneration techniques developed in recent years. By providing a mechanism of fabricating custom-fit and patient-specific biodegradable implants to support the regeneration of mineralized tissue, stereolithography is arguably one of the primary enabling technologies promoting advancements in this field.

4.3 Stereolithographic Fabrication for Cartilage Tissue Engineering

Many of the pioneering advances in tissue engineering have targeted applications in tissue engineering of cartilage, since this type of tissue is often relatively homogeneous and largely avascular, and hence relatively easy to fabricate. The ability to regenerate load-bearing and articular cartilaginous tissues can address many ongoing challenges in replacing tissues damaged by degenerative diseases such as progressive arthritis, aging, or traumatic injury [85].

4.3.1 Cosmetic Tissue-Engineered Cartilage

Reminiscent of the external maxillofacial prosthetics discussed earlier in this chapter, Naumann et al. used a combination of CT and UV laser-based stereolithographic fabrication to fabricate three-dimensional bioresorbable scaffolds for tissue engineering of an auricle from the hyaluronic acid derivative Hyaff 11 [86]. As hyaluronan is an important component of native cartilage, this resin was chosen and tailored to suit the particular application targeted by this study. Histomorphology and immunohistochemistry performed on Hyaff 11 scaffolds seeded with living chondrocytes demonstrated the homogeneous expression of cartilage-specific collagen type II within the engineered tissue after 4 weeks of *in vitro* culture at physiologic conditions (Fig. 6.23).

4.3.2 Load-Bearing Tissue-Engineered Cartilage

Other resins used for tissue engineering of cartilage have been chosen for the close match between their material properties, such as water uptake and swelling depth, and mechanical properties, such as stiffness, and those of native cartilage tissue. For applications in tissue engineering of load-bearing cartilage, such as that found in intervertebral discs, match of the material and mechanical properties of regenerated and native tissue is of utmost importance in functional output. Cho and coworkers targeted this challenge by manufacturing biodegradable scaffolds from TMC-based oligomers, whose material and mechanical properties match those of native cartilage [33]. Chondrocytes extracted from articular cartilage and seeded within these scaffolds were cultured at physiologic conditions and supplemented with transforming growth factor (TGF) and insulin-like growth factor. Viability of cells over 2 weeks was determined by a quantitative measure of the mitochondrial metabolic activity of adhered cells (3-(4,5-dimethylthiazol-2-yl)-2,5-diphenyltetrazolium bromide assay), showing strong adhesion and activity of seeded chondrocytes.

4.3.3 "Bottom–Up" Fabrication of Tissue-Engineered Cartilage

Ellisseeff and coworkers improved upon these scaffold-based fabrication techniques by incorporating a suspension

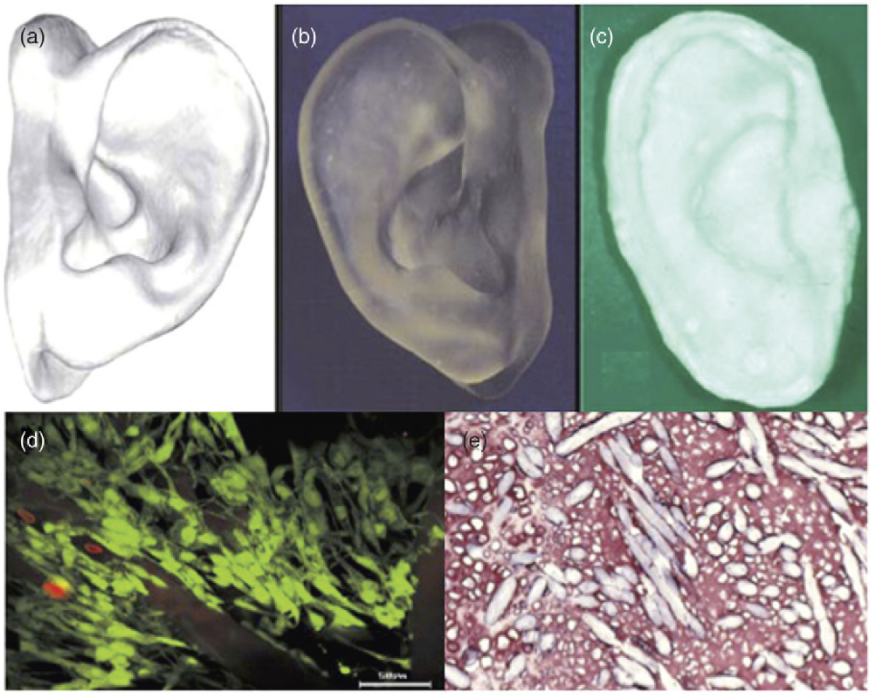

FIGURE 6.23 Cosmetic tissue engineered cartilage. (a) CAD model of contralateral (i.e., undamaged) ear; (b) Stereolithographic fabrication of mirror image design; (c) bioresorbable hyoluronan-based scaffold fabricated with the aid of stereolithography; (d) confocal microscopy of scaffold after 4 weeks *in vitro* culture showing homogeneous distribution of vital chondrocytes (green) distributed throughout scaffold, with relatively few avital cells (red); (e) histomorphology and immunohistochemistry of chondrocyte constructs after 4 weeks *in vitro* culture showing homogenous expression of cartilage-specific collagen type II [86].

of embryonic stem cells that had formed embryoid bodies (EB) into a photosensitive PEG hydrogel-based prepolymer solution [87]. A simple UV light and a physical mask-based SLA was used to encapsulate EBs into a three-dimensional architecture and cultured *in vitro* in chondrogenic medium containing (TGF)- β1, and bone morphogenic protein-2. Extensive characterization of regenerated tissue fabricated in this manner via gene expression and protein analysis as well as histological analysis, suggest that EBs encapsulated in these hydrogels via stereolithography up-regulated cartilage-relevant markers and induced a chondrocytic phenotype. The basophilic exctracellular matrix deposited in the engineered 3D environment was characteristic of neocartilage, suggesting that this apparatus is a promising approach to engineering complex functional replacements for native cartilage.

4.4 Stereolithographic Fabrication for Cardiac and Vascular Tissue Engineering

The increasing prevalence of cardiovascular disease, which is the primary cause of death in the United States and other developing countries, motivates the development of tissue-engineered replacements for tissues in the cardiovascular system. Moreover, advancements pertaining to the regeneration of interconnected vascular networks are broadly applicable to all regenerative medicine applications. Vascularization of engineered tissues, which is the key challenge facing researchers aiming to create large-scale replacements for native tissue and organs, must be addressed before regenerative medicine technologies are adapted for widespread clinical use [88].

4.4.1 2D Cardiac Tissue Engineering

As cardiac tissue is inherently an actuator in the body, advances in tissue engineering of cardiac muscle powered actuators have many applications in restoring pulsatile/beating function to damaged or ischemic cardiac tissue. Bashir and coworkers fabricated protein surface functionalized hydrogel cantilever-like substrates via a laser-based stereolithographic 3D printing apparatus and seeded primary cardiomyocytes derived from neonatal rats upon these 2D scaffolds [89]. The cardiomyocytes formed a connected cell sheet attached to the substrate and were able to drive actuation of the hydrogel substrate via contraction of the engineered tissue (Fig. 6.24).

4.4.2 3D Cardiac Tissue Engineering

Sodian et al. explored 3D scaffolds for cardiac tissue engineering by fabricating stereolithographic plastic models for thermoplastic modeling of two elastomers, poly-4-hydroxybutyrate and polyhydroxyoctanoate, in the shape

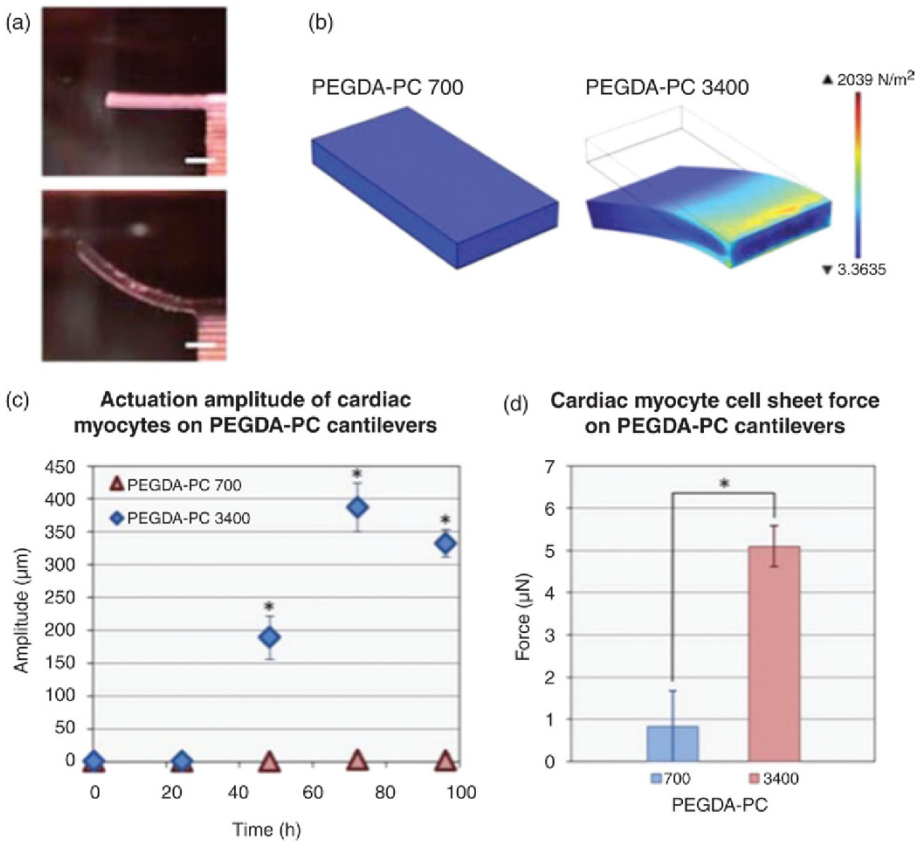

FIGURE 6.24 **2D engineered cardiac tissue manufactured with the aid of stereolithography.** (a) Primary neonatal cardiomyocytes seeded on PEG-based cantilevers of high stiffness (top) and low stiffness (bottom) fabricated via stereolithography; (b) computer aided simulation showing the distribution of stresses in the prototyped cantilevers as a result of contraction of the engineered cell sheet; (c) actuation amplitude of cardiac myocytes on PEG-based cantilevers; (d) force exerted by the engineered cardiac myocyte cell sheet [89].

of a trileaflet heart valve scaffold [90]. These valve scaffolds were placed inside a bioreactor and subjected to pulsatile flow, and demonstrated synchronous opening and closing behaviors similar to those seen *in vitro*. This technique, rendered feasible by stereolithography, demonstrates the ability to accurately reconstruct physiological valve design and bypassing the need for a human allograft.

Butcher and coworkers demonstrated further improvements on this technology by combining stereolithographic fabrication and bioplotting technologies to generate 3D cardiac tissue scaffolds for manufacturing heterogeneous aortic valves. PEGDA hydrogels were supplemented with alginate and cured by an UV LED crosslinking module, demonstrating a broadly tunable range of mechanical properties for printed valve scaffolds. Porcine aortic valve interstitial cells seeded within these scaffolds and cultured *in vitro* at physiologic conditions for 21 days showed cell viability and spreading on this biocompatible fabricated scaffold (Fig. 6.25).

4.4.3 *Vascular Tissue Engineering*

Kong and coworkers demonstrated the use of a direct laser-writing apparatus to fabricate "Living" microvascular stamps that could controllably pattern functional neovessels when tested *in ovo* on the chick chorioallantoic membrane [92]. These SLA-fabricated stamps, comprised of fibroblasts encapsulated in PEG-based hydrogels that were stimulated to secrete the angiogenic molecule vascular endothelial growth factor (VEGF), proved to demonstrate orchestrated control over the placement and geometry of neovasculature.

Work by Khademhosseini and coworkers extended this work by fabricating very-high-resolution three-dimensional porous scaffold architectures with intricate geometries using a projection stereolithography system [49]. The mechanical properties of these 3D scaffolds were tuned and regulated by varying the chemical composition of the GelMA resins used as photosensitive prepolymers in this study. The complex interconnected pore structure rendered feasibly via stereolithographic fabrication led to the formation of a high cell-density network of seeded human umbilical vein endothelial cells (HUVECs) within the scaffold. Immunohistochemistry of these tissue-engineered substitutes showed that seeded cells maintained their endothelial phenotype over time and were well distributed throughout the scaffold during the observed culture period, thereby demonstrating a promising method of engineering 3D

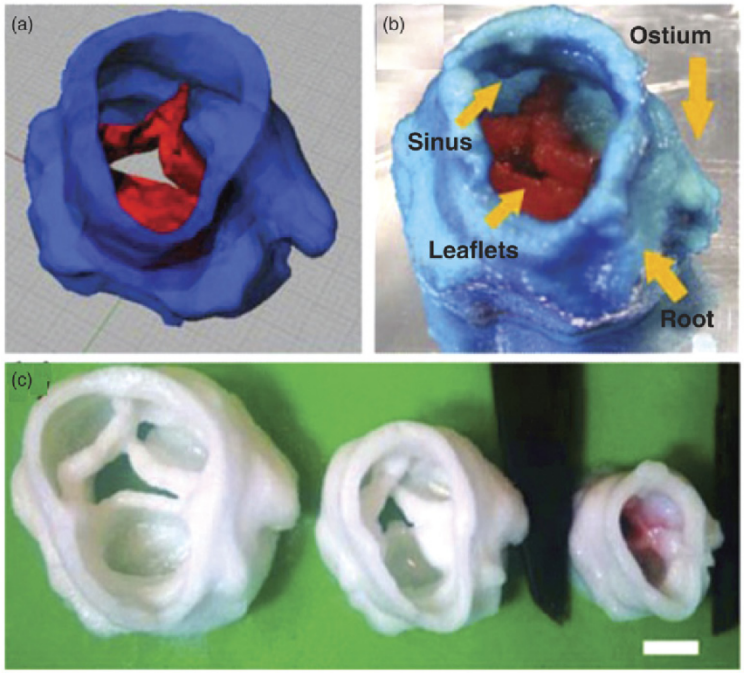

FIGURE 6.25 3D tissue-engineered aortic valve. (a) Porcine aortic valve model; (b) printed aortic valve model formed from PEG-based resins. Root (blue) formed from stiffer hydrogel and leaflets formed from less stiff hydrogel; (c) aortic valve scaffolds printed at different scales (Inner diameter = 22, 17, and 12 mm) for shape fidelity and resolution analysis [91].

vascular networks within SLA-fabricated tissue constructs (Fig. 6.26).

4.5 Stereolithographic Fabrication for Other Tissue Engineering Applications

SLA-based technologies are broadly applicable in a vast array of tissue engineering applications. The techniques used for fabrication are the same across tissue types, but the types of chemically modified resins and 3D macro- and microscale architectures have been modified to suit the specific application in question. A couple notable examples that use next-generation multiphoton SLA processes are mentioned in this section.

4.5.1 *Liver Tissue Engineering*

Wan and coworkers fabricated three-dimensional microstructure scaffolds for tissue engineering of liver using a two-photon laser scanning photolithography technique [93]. In this study, a commercially available photocurable polymer manufactured by 3D systems (the company that pioneered stereolithographic fabrication) was selectively polymerized using laser pulses. Sterilized scaffolds were then functionalized with collagen and seeded with primary rat hepatocytes. To assess for liver-specific function of the engineered tissue, the culture medium was assayed for albumin and urea secretion and demonstrated that the cells had received adequate nutrient transport within the fabricated scaffolds and were able to preserve their functionality.

4.5.2 *Neural Tissue Engineering*

Claeyssens and coworkers used a novel multiphoton polymerization approach to fabricate polylactide-based scaffolds for neural tissue engineering [94]. The photosensitive polylactide resin (PLA) was cured using femtosecond laser pulses of IR irradiation, with a maximum resolution of 800 nm achieved for scaffold feature sizes. Neuroblastoma cells were cultured on these structured PLA scaffolds, demonstrating cell viability and proliferation on scaffolds to provide proof of the biocompatibility of these structures (Fig. 6.27).

The examples listed in this section are just a few of the many studies that serve as strong demonstrations of the potential of stereolithographic fabrication technologies to suit a wide variety of applications in tissue engineering and regenerative medicine.

5 CONCLUSIONS

5.1 Current Challenges in Stereolithographic Fabrication

5.1.1 *Multimaterial Fabrication*

One of the primary challenges facing widespread adaptation of stereolithography for a vast array of translational

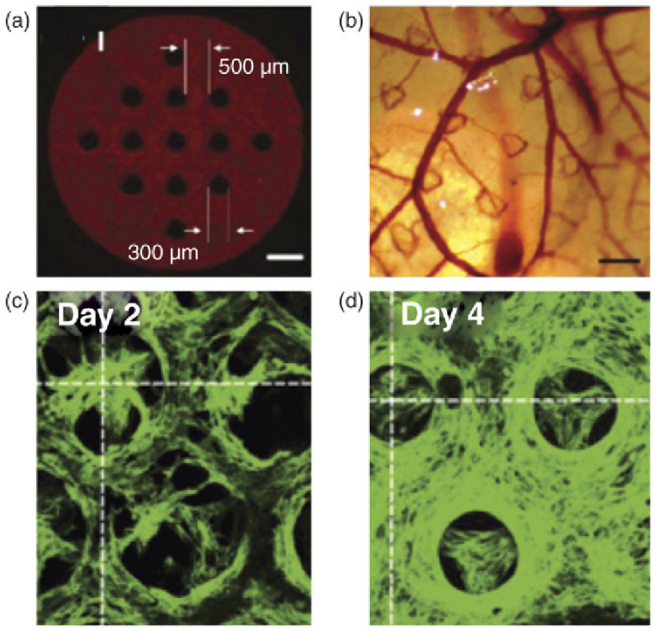

FIGURE 6.26 **Tissue engineered vasculature is required to create large-scale replacements for any tissue/organ system.** (a) Hydrogel patch containing VEGF-secreting fibroblasts fabricated via stereolithography; (b) patterned formation of neovasculature in response to *in ovo* incubation of the hydrogel on the chick chorioallantoic membrane; (c, d) adhesion and spreading of HUVECs on GelMA scaffold fabricated via stereolithography shown Day 2 and Day 4 postseeding. *(Figure 6.26a,b reprinted with permission from Jeong et al. [92]; Figure 6.26c,d reprinted with permission from Gauvin et al. [49].).*

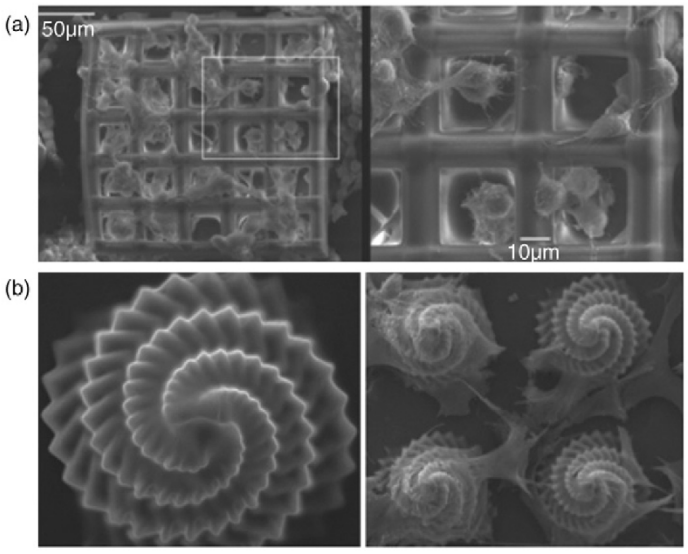

FIGURE 6.27 **Neural tissue engineering.** (a) 3D microscaffolds manufactured via multiphoton stereolithography using a PLA resin. Neuroblastoma cells cultured within these scaffolds demonstrate excellent adhesion and spreading 5 days postseeding; (b) complex microscale architectures, such as seashells, can be printed using stereolithography and used to control the directional spreading of seeded cells [94].

biomedical applications is the difficulty of fabricating multimaterial 3D structures. Wicker and coworkers demonstrated wash/refill steps that could be employed to fabricate 3D multimaterial structures with a projection micro-SLA [8]. Bashir and coworkers extended this work to encapsulate multiple cell types in 3D patterned hydrogels using a single photon laser-based SLA [42]. This approach, while efficacious, causes a significant increase in part build-times. Build time can be reduced by employing automated syringe-pump systems for washing/filling resins. Arcaute et al. recently proposed an alternative method for fabrication using multiple resins by employing the use of an array of "minivats," which allow for selective spatially controlled variation of material composition in 3D architectures [95].

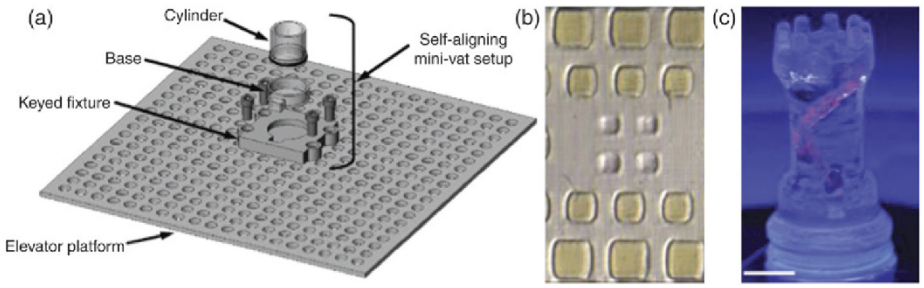

FIGURE 6.28 Multimaterial fabrication is one of the primary challenges facing stereolithography. (a) Schematic of self-aligning minivat setup proposed by Arcaute et al.; (b) spatially controlled variation of resin within a single printed layer; (c) complex 3D chess rook structure with fluorescent internal staircase manufactured using this multimaterial stereolithographic fabrication approach [95].

Further advancements of this and other multimaterial strategies promise to remove the limitation from stereolithographic biofabrication (Fig. 6.28).

5.1.2 Microscale Control of Architecture

The limitations posed by the difficulty of multimaterial fabrication are mainly contingent on the resultant inability to create precise predefined spatial patterns of mechanical, material, and biochemical properties within 3D structures. For tissue engineering applications, the processes currently in common use do not allow for accurate placement of single cells or bioactive molecules in predefined locations. Rather, cells and molecules are mixed within resins, assumed to be uniformly mixed, and then selectively polymerized prior to washing and refilling steps. Advances in various single-cell and molecule manipulation technologies may address some of the main concerns regarding this limitation of stereolithographic biofabrication.

Timp and coworkers addressed this challenge by using optical tweezers to selectively manipulate single cells into precisely defined 3D spatial positions within a prepolymer solution prior to encapsulation via photopolymerization [96]. This approach, while effective, would prove to be extremely time consuming for the fabrication of large 3D structures containing millions of cells and biomolecules. Bashir and coworkers have demonstrated a higher throughput approach based on the principle of dielectrophoresis (DEP). In this process, a set of electrodes is incorporated on the build platform of a single photon SLA, allowing for selective and simultaneous patterning of large arrays of cells prior to photopolymerization [97] (Fig. 6.29).

Pioneering work in this field has recently been published by Deforest and Anseth, who have demonstrated hydrogels with tunable range of properties (mechanical, material, biochemical, etc.) that can be spatiotemporally controlled with high 3D resolution [98]. This spatiotemporal control is accomplished via a novel cytocompatible "click-based" chemistry that uses wavelength-specific photochemical reactions to dynamically conjugate or cleave bioactive moieties to 3D cell-culture systems *in vitro* (Fig. 6.30).

5.2 New Developments in Stereolithography for Biomedical Applications

Stereolithographic technologies have enabled the rise of reverse-engineering native tissue for applications in regenerative medicine, but this is not the only field of research opened up by work in this area. By giving researchers the ability to build systems of cells, stereolithography has opened up the possibility of designing novel systems that harness the innate dynamic abilities of cells to self-organize and respond to environmental cues. This idea of forward-engineering integrated cellular systems, or "biological machines," with multiple functionalities using stereolithography as an enabling tool has many potential applications.

Bashir and coworkers have recently designed a biological machine, or "biobot," that utilizes the autonomous and synchronous contraction of engineered cardiac tissue to power locomotion of an SLA-fabricated soft robotic device [99]. Further studies in this field that focus on creating biological machines that can accomplish such objectives of robotics as sensing, storage, and processing of signals, and a resultant response (such as actuation) have many potential applications. Biological machines that dynamically respond to environmental cues can target a diverse set of translational medical applications including drug-delivery, noninvasive surgery, dynamic implants, and biocompatible microelectronics. These machines and other studies that build upon them will demonstrate the power using SLA fabrication and cells as building blocks to engineer the machines and systems of the future.

5.3 Stereolithographic 3D Bioprinting for Biomedical Applications

The future of modern medicine is undoubtedly rooted in the core philosophy of customized/personalized healthcare.

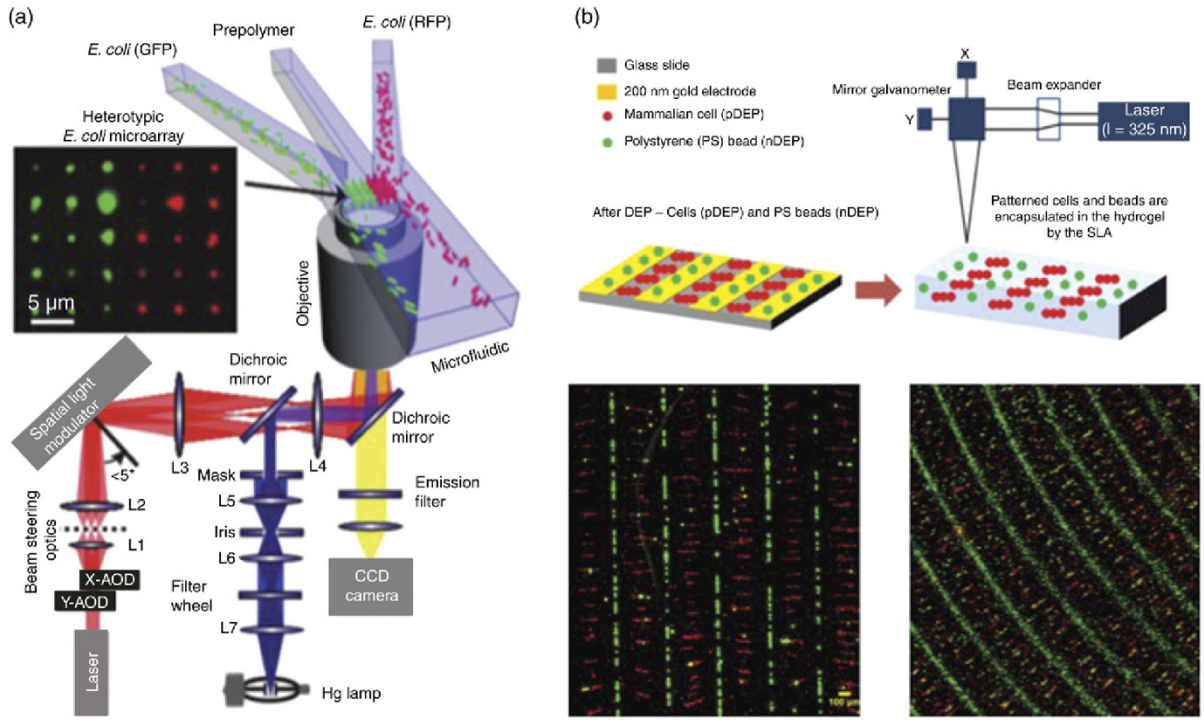

FIGURE 6.29 **High-resolution patterning of single cells within a complex 3D structure is a major challenge facing stereolithography.** (a) Optical tweezers used to precisely manipulate arrays of fluorescently labeled *Escherichia coli* before encapsulation within a photosensitive polymer [96]; (b) DEP used as a high-throughput approach to manipulating fluorescently labeled cells and beads into precisely defined spatial patterns prior to encapsulation in a photosensitive polymer [97].

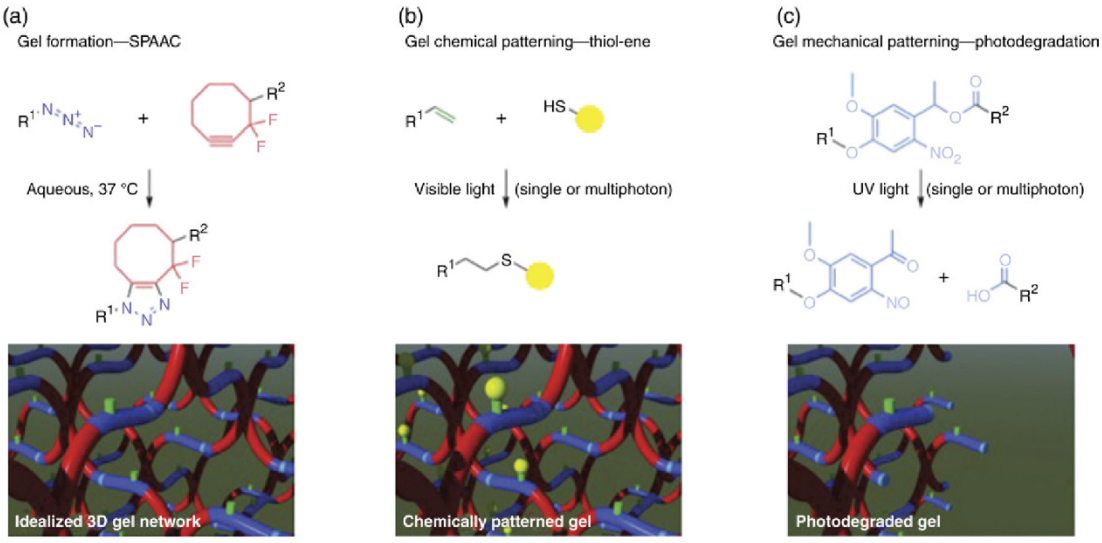

FIGURE 6.30 **High-resolution spatiotemporal control of mechanical, material, and biochemical properties within a 3D structure is the next-generation requirement for stereolithographic fabrication.** (a) Formation of a 3D hydrogel; (b) single or multiphoton visible light used to chemically pattern bioactive moieties within a 3D hydrogel matrix; (c) single or multiphoton UV light used to selectively degrade portions of the polymerized gel [98].

As we learn more about the underlying design principles and molecular mechanisms governing biological systems, we can develop precisely individualized and targeted cures that address patient-specific needs. This motivates the need for developing an enabling technology that allows us to fabricate complex 3D structures that are biocompatible, biodegradable, and bioactive. Such biofabricated structures can readily integrate with a host biological system to perform a specified task, such as targeting diseased tissues and promoting tissue regeneration.

Over the past few decades, stereolithographic fabrication technologies have advanced greatly in the quality, resolution, and accuracy of manufactured parts. Recent developments in creating photocurable resins that are biocompatible, biodegradable, and bioactive have enabled a vast array of biomedical and translation medical applications of SLA-based fabrication technologies. In a progressive manner that mimics the progression of the medical field itself, SLA machines have been used to manufacture: (1) data visualization and surgical planning tools to aid clinicians; (2) individualized prosthetics; (3) customized implants and surgical tools; (4) biomaterial scaffolds for tissue engineering; and (5) high-density cellular constructs for tissue engineering. In each of these broad types of applications, stereolithographic techniques have been readily integrated with medical imaging technologies (MRI, CT) in order to improve disease diagnosis, preoperative planning, quality and morphology of prosthetics and implants, and functional success of complex surgeries. Furthermore, SLA has established itself as one of the primary enabling tools that will be useful for regenerative medicine applications in the coming years.

Limitations of stereolithographic systems, such as the difficulties involved with multimaterial construct fabrication and high-resolution spatiotemporal control over the placement of specific moieties within complex 3D structures, are being addressed by advances in SLA technologies (projection stereolithography, multiphoton methods, automated resin dispersal systems, arrays of multimaterial "minivats," etc.) as well as advances in novel resin chemistries (dynamic photoconjugation and photocleavage of moieties within 3D structures). New biodegradable and bioactive resins continue to be developed as this technology achieves even broader use in the field of biomedical engineering.

As a whole, the versatility in design, scale, resolution, and broad applicability of stereolithographic technologies render them the ideal enabling technology for biomedical and translational medical applications.

GLOSSARY

Bioactive A term used to describe a substance or material that has a biological effect on a living cell, tissue, or organism.

Biocompatible A term used to describe a substance or material that is not harmful to living cells, tissues, or organisms.

Biodegradable A term used to describe a substance or material that can be decomposed by a living cell, tissue, or organism.

Cytotoxic A term used to describe a substance that is toxic to living cells.

Elastomer A material that is compliant or flexible, that is, characterized by a low Young's Modulus and relatively high failure strain.

Hydrogel Term describing a broad class of hydrophilic materials that are highly absorbent and have mechanical properties similar to native tissue.

Photoinitiator A reactive chemical compound that decomposes to form high-energy free radicals, or molecules with unpaired valence electrons, when exposed to light.

Photosensitive Prepolymer (Photopolymer) A solution composed of a polymer and a photoinitiator that can be excited into a radical state through exposure to light and driven to cure into a solid or gel-like structure.

Resin General descriptive term for a photosensitive prepolymer that is used for fabrication using a SLA.

Stereolithography A subset of additive manufacturing technology that relies on using light to cure a photosensitive prepolymer.

ABBREVIATIONS

BMP	Bone morphogenic protein
CAD	Computer-aided design
CHO	Chinese hamster ovary
CT	Computed tomography
DEF	Diethyl fumarate
DEP	Dielectrophoresis
DMD	Digital micromirror device
ECM	Extracellular matrix
EB	Embryoid body
GelMA	Gelatin methacrylate
gMSC	Gingival mesenchymal stem cells
hFOB	Human fetal osteoblastic cells
hMSC	Human mesenchymal stem cells
HUVEC	Human umbilical vein endothelial cells
IR	Infrared
LAP	Lithium phenyl-2,4,6-trimethylbenzoylphosphinate
LVEC	Large vessel endothelial cells
MRI	Magnetic resonance imaging
NIH/3T3	Mouse fibroblast cell line
NVP	*N*-Vinyl-2-pyrrolidone
PDLLA	Poly(D,L-lactide)
PEG	Poly(ethylene glycol)
PEGDMA	Poly(ethylene glycol) dimethacrylate
PLA	Polylactide
PPF	Poly(propylene fumarate)
RGDS	Arg–Gly–Asp–Ser tetrapeptide
SEM	Scanning electron microscopy
SIRC	Statens seruminstitut rabbit corneal cells
SLA	Stereolithography apparatus
TGF	Transforming growth factor
TMC	Trimethylene carbonate
UV	Ultraviolet
VEGF	Vascular endothelial growth factor

ACKNOWLEDGMENTS

We thank our funding sources: National Science Foundation (NSF) Science and Technology Center (STC) Emergent Behavior of Integrated Cellular Systems (EBICS) Grant CBET-0939511, the National Science Foundation (NSF) Grant 0965918 IGERT: Training the Next Generation of Researchers in Cellular and Molecular Mechanics and Bio-Nanotechnology, and National Science Foundation (NSF) Graduate Research Fellowship Program (GRFP) Grant DGE-1144245.

REFERENCES

[1] Melchels FPW, Feijen J, Grijpma DW. A review on stereolithography and its applications in biomedical engineering. Biomaterials 2010;31:6121–30.

[2] Pham D, Gault R. A comparison of rapid prototyping technologies. Int J Mach Tools Manuf 1998;38:1257–87.

[3] Yang S, Leong K-F, Du Z, Chua CK. The design of scaffolds for use in tissue engineering. Part II. Rapid prototyping techniques. Tissue Eng 2002;8:1–11.

[4] Wendel B, Rietzel D, Kühnlein F, Feulner R, Hülder G, Schmachtenberg E. Additive processing of polymers. Macromol Mater Eng 2008;293:799–809.

[5] Bartolo PJ. Stereolithographic Processes. In: Bártolo PJ, editor. Stereolithography: materials, processes and applications. Boston, MA: Springer US; 2011. p. 1–36.

[6] Johnson DW, Sherborne C, Didsbury MP, Pateman C, Cameron NR, Claeyssens F. Macrostructuring of emulsion-templated porous polymers by 3D laser patterning. Adv Mater 2013;25:3178–3181.

[7] Han L-H, Mapili G, Chen S, Roy K. Projection microfabrication of three-dimensional scaffolds for tissue engineering. J Manuf Sci Eng 2008;130. 021005.

[8] Choi J-W, MacDonald E, Wicker R. Multi-material microstereolithography. Int J Adv Manuf Technol 2009;49:543–51.

[9] Maruo S, Nakamura O, Kawata S. Three-dimensional microfabrication with two-photon-absorbed photopolymerization. Opt Lett 1997;22:132–4.

[10] Lee KS, Kim RH, Yang DY, Park SH. Advances in 3D nano/microfabrication using two-photon initiated polymerization. Prog Polym Sci 2008;33:631–81.

[11] Farsari M, Filippidis G, Drakakis TS, Sambani K, Georgiou S, Papadakis G, et al. Three-dimensional biomolecule patterning. Appl Surf Sci 2007;253:8115–8.

[12] Weiß T, Hildebrand G, Schade G, Liefeith K. Two-photon polymerization for microfabrication of three-dimensional scaffolds for tissue engineering application. Eng Life Sci 2009;9:384–90.

[13] Ovsianikov A, Gruene M, Pflaum M, Koch L, Maiorana F, Wilhelmi M, et al. Laser printing of cells into 3D scaffolds. Biofabrication 2010;2. 014104.

[14] Tondiglia VP, Natarajan LV, Sutherland RL, Tomlin D, Bunning TJ. Holographic formation of electro-optical polymer-liquid crystal photonic crystal. Adv Mater 2002;14:187–91.

[15] Moon JH, Ford J, Yang S. Fabricating three-dimensional polymeric photonic structures by multi-beam interference lithography. Polym Adv Technol 2006;17:83–93.

[16] Ullal CK, Maldovan M, Thomas EL, Chen G, Han Y-J, Yang S. Photonic crystals through holographic lithography: simple cubic, diamond-like, and gyroid-like structures. Appl Phys Lett 2004;84:5434.

[17] Heller C, Schwentenwein M, Russmueller G, Varga F, Stampfl J, Liska R. Vinyl esters: low cytotoxicity monomers for the fabrication of biocompatible 3D scaffolds by lithography based additive manufacturing. J Polym Sci Part A1 Polym Chem 2009;47:6941–54.

[18] Davis FJ, Mitchell GR. Polymeric materials for rapid manufacturing. Stereolithography: materials, processes and applications. New York, NY: Springer; 2011. p. 113–39.

[19] Williams CG, Malik AN, Kim TK, Manson PN, Elisseeff JH. Variable cytocompatibility of six cell lines with photoinitiators used for polymerizing hydrogels and cell encapsulation. Biomaterials 2005;26:1211–8.

[20] Fairbanks BD, Schwartz MP, Bowman CN, Anseth KS. Photoinitiated polymerization of PEG-diacrylate with lithium phenyl-2,4,6-trimethylbenzoylphosphinate: polymerization rate and cytocompatibility. Biomaterials 2009;30:6702–7.

[21] Popov VK, Evseev AV, Ivanov AL, Roginski VV, Volozhin AI, Howdle SM. Laser stereolithography and supercritical fluid processing for custom-designed implant fabrication. J Mater Sci Mater Med 2004;15:123–8.

[22] Chu GT-M, Brady GA, Miao W, Halloran JW, Hollister SJ, Brei D. Ceramic SFF by direct and indirect stereolithography. In: Materials Research Society Symposium; 1999: 119–123.

[23] Provin C, Monneret S, Chimie D De. Complex ceramic-polymer composite microparts made by microstereolithography. In: Proceedings of SPIE;2001: 535–542.

[24] Licciulli A, Esposito Corcione C, Greco A, Amicarelli V, Maffezzoli A. Laser stereolithography of ZrO_2 toughened Al_2O_3. J Eur Ceram Soc 2005;25:1581–9.

[25] Chu TMG, Orton DG, Hollister SJ, Feinberg SE, Halloran JW. Mechanical and *in vivo* performance of hydroxyapatite implants with controlled architectures. Biomaterials 2002;23:1283–93.

[26] Hinczewski C, Corbel S, Chartie T. Ceramic suspensions suitable for stereolithography. J Eur Ceram Soc 1998;18:583–90.

[27] Jansen J, Melchels FPW, Grijpma DW, Feijen J. Fumaric acid monoethyl ester-functionalized poly (D,L-lactide)/*N*-vinyl-2-pyrrolidone resins for the preparation of tissue engineering scaffolds by stereolithography. Biomacromolecules 2009;10:214–20.

[28] Lee K-W, Wang S, Fox BC, Ritman EL, Yaszemski MJ, Lu L. Poly(propylene fumarate) bone tissue engineering scaffold fabrication using stereolithography: effects of resin formulations and laser parameters. Biomacromolecules 2007;8:1077–84.

[29] Bens A, Seitz H, Bermes G, Emons M. Non-toxic flexible photopolymers for medical stereolithography technology. Rapid Prototyp J 2007;13:38–47.

[30] Matsuda T, Mizutani M, Arnold SC. Molecular design of photocurable liquid biodegradable copolymers. 1. Synthesis and photocuring characteristics. Macromolecules 2000;33:795–800.

[31] Matsuda T, Mizutani M. Molecular design of photocurable liquid biodegradable copolymers. 2. Synthesis of coumarin-derivatized oligo(methacrylate)s and photocuring. Macromolecules 2000;33:791–4.

[32] Matsuda T, Mizutani M. Liquid acrylate-endcapped biodegradable poly(epsilon-caprolactone-co-trimethylene carbonate). II. Computer-aided stereolithographic microarchitectural surface photoconstructs. J Biomed Mater Res 2002;62:395–403.

[33] Lee SJ, Kang HW, Park JK, Rhie JW, Hahn SK, Cho DW. Application of microstereolithography in the development of three-dimensional cartilage regeneration scaffolds. Biomed Microdevices 2008;10:233–41.

[34] Cooke MN, Fisher JP, Dean D, Rimnac C, Mikos AG. Use of stereolithography to manufacture critical-sized 3D biodegradable scaffolds for bone ingrowth. J Biomed Mater Res B Appl Biomater 2002;64:65–9.

[35] Lee JW, Lan PX, Kim B, Lim G, Cho D-W. 3D scaffold fabrication with PPF/DEF using micro-stereolithography. Microelectron Eng 2007;84:1702–5.

[36] Choi JW, Wicker R, Lee SH, Choi KH, Ha CS, Chung I. Fabrication of 3D biocompatible/biodegradable micro-scaffolds using dynamic mask projection microstereolithography. J Mater Process Technol 2009;209:5494–503.

[37] Melchels FPW, Feijen J, Grijpma DW. A poly(D,L-lactide) resin for the preparation of tissue engineering scaffolds by stereolithography. Biomaterials 2009;30:3801–9.
[38] Stampfl J, Liska R. Polymerizable hydrogels for rapid prototyping: chemistry, photolithography, and mechanical properties. In: Bártolo PJ, editor. Stereolithography: materials, processes and applications. Boston, MA: Springer US; 2011. p.161–182.
[39] Hinkley JA, Morgret LD, Gehrke SH. Tensile properties of two responsive hydrogels. Polymer 2004;45:8837–43.
[40] Dhariwala B, Hunt E, Boland T. Rapid prototyping of tissue-engineering constructs, using photopolymerizable hydrogels and stereolithography. Tissue Eng 2004;10:1316–22.
[41] Arcaute K, Mann BK, Wicker RB. Stereolithography of three-dimensional bioactive poly(ethylene glycol) constructs with encapsulated cells. Ann Biomed Eng 2006;34:1429–41.
[42] Chan V, Zorlutuna P, Jeong JH, Kong H, Bashir R. Three-dimensional photopatterning of hydrogels using stereolithography for long-term cell encapsulation. Lab Chip 2010;10:2062–70.
[43] Lee SH, Moon JJ, West JL. Three-dimensional micropatterning of bioactive hydrogels via two-photon laser scanning photolithography for guided 3D cell migration. Biomaterials 2008;29:2962–8.
[44] Northen TR, Brune DC, Woodbury NW. Synthesis and characterization of peptide grafted porous polymer microstructures. Biomacromolecules 2006;7:750–4.
[45] Chan V, Collens MB, Jeong JH, Park K, Kong H, Bashir R. Directed cell growth and alignment on protein-patterned 3D hydrogels with stereolithography. Virtual Phys Prototyp 2012;7:219–28.
[46] Mapili G, Lu Y, Chen S, Roy K. Laser-layered microfabrication of spatially patterned functionalized tissue-engineering scaffolds. J Biomed Mater Res B Appl Biomater 2005;75:414–24.
[47] Schuster M, Turecek C, Weigel G, Saf R, Stampfl J, Varga F, et al. Gelatin-based photopolymers for bone replacement materials. J Polym Sci Part A1 Polym Chem 2009;47:7078–89.
[48] Zimmerman J, Bittner K, Stark B, Mulhaupt R. Novel hydrogels as supports for *in vitro* cell growth: poly(ethylene glycol)- and gelatine-based (meth)acrylamidopeptide macromonomers. Biomaterials 2002;23:2127–34.
[49] Gauvin R, Chen YC, Lee JW, Soman P, Zorlutuna P, Nichol JW, et al. Microfabrication of complex porous tissue engineering scaffolds using 3D projection stereolithography. Biomaterials 2012;33:3824–34.
[50] Smeds KA, Pfister-Serres A, Hatchell DL, Grinstaff MW. Synthesis of a novel polysaccharide hydrogel. J Macromol Sci Part A Pure Appl Chem 1999;36:981–9.
[51] Qiu Y, Zhang N, Kang Q, An Y, Wen X. Chemically modified light-curable chitosans with enhanced potential for bone tissue repair. J Biomed Mater Res A 2009;89:772–9.
[52] Gebinoga M, Katzmann J, Fernekorn U, Hampl J, Weise F, Klett M, et al. Multiphoton structuring of native polymers: a case study for structuring natural proteins. Eng Life Sci 2013;13:368–375.
[53] Zorlutuna P, Jeong JH, Kong H, Bashir R. Stereolithography-based hydrogel microenvironments to examine cellular interactions. Adv Funct Mater 2011;21:3642–51.
[54] Schuster M, Turecek C, Kaiser B, Stampfl J, Liska R, Varga F. Evaluation of biocompatible photopolymers I: photoreactivity and mechanical properties of reactive diluents. J Macromol Sci Part A 2007;44:547–57.
[55] Schuster M, Turecek C, Mateos A, Stampfl J, Liska R, Varga F. Evaluation of biocompatible photopolymers II: further reactive diluents. Monatshefte für Chemie – Chem Mon 2007;138:261–8.
[56] Seitz H, Tille C, Irsen S, Bermes G, Sader R, Zeilhofer H-F. Rapid prototyping models for surgical planning with hard and soft tissue representation. Int Congr Ser 2004;1268:567–72.
[57] Mankovich NJ, Cheeseman AM, Stoker NG. The display of three-dimensional anatomy with stereolithographic models. J Digit Imaging 1990;3:200–3.
[58] Bill JS, Reuther JF, Dittmann W, Kübler N, Meier JL, Pistner H, et al. Stereolithography in oral and maxillofacial operation planning. Int J Oral Maxillofac Surg 1995;24:98–103.
[59] Sarment DP, Al-Shammari K, Kazor CE. Stereolithographic surgical templates for placement of dental implants in complex cases. Int J Periodontics Restorative Dent 2003;23:287–95.
[60] De Momi E, Pavan E, Motyl B, Bandera C, Frigo C. Hip joint anatomy virtual and stereolithographic reconstruction for preoperative planning of total hip replacement. Int Congr Ser 2005;1281:708–12.
[61] Binder TM, Moertl D, Mundigler G, Rehak G, Franke M, Delle-Karth G, et al. Stereolithographic biomodeling to create tangible hard copies of cardiac structures from echocardiographic data: *in vitro* and *in vivo* validation. J Am Coll Cardiol 2000;35:230–7.
[62] Goiato MC, Santos MR, Pesqueira AA, Moreno A, dos Santos DM, Haddad MF. Prototyping for surgical and prosthetic treatment. J Craniofac Surg 2011;22:914–7.
[63] El-Siblani A. Advantages of utilizing DMD based rapid manufacturing systems in mass customization applications. Proc SPIE 2010;7596:75960G1–175960G.
[64] Coward TJ, Watson RM, Wilkinson IC. Fabrication of a wax ear by rapid process modeling using stereolithography. Int J Prosthodont 1999;12:20–7.
[65] Runte C, Dirksen D, Deleré H, Thomas C, Runte B, Meyer U, et al. Optical data acquisition for computer-assisted design of facial prostheses. Int J Prosthodont 2002;15:129–32.
[66] Freeman D, Wontorcik L. Stereolithography and prosthetic test socket manufacture: a cost/benefit analysis. J Prosthetics Orthot 1998;10:17–20.
[67] D'Urso PS, Earwaker WJ, Barkert TM, Redmond MJ, Thompson RG, Effeney DJ, et al. Custom cranioplasty using stereolithography and acrylic. Br J Plast Surg 2000;53:200–4.
[68] Wurm G, Tomancok B, Holl K, Trenkler J. Prospective study on cranioplasty with individual carbon fiber reinforced polymer (CFRP) implants produced by means of stereolithography. Surg Neurol 2004;62:510–21.
[69] Morris CL, Barber RF, Day R. Orofacial prosthesis design and fabrication using stereolithography. Aust Dent J 2000;45:250–3.
[70] Liska WD, Marcellin-Little DJ, Eskelinen EV, Sidebotham CG, Harrysson OLA, Hielm-Bjorkman AK. Custom total knee replacement in a dog with femoral condylar bone loss. Vet Surg 2007;36:293–301.
[71] Minns RJ, Bibb R, Banks R, Sutton RA. The use of a reconstructed three-dimensional solid model from CT to aid the surgical management of a total knee arthroplasty: a case study. Med Eng Phys 2003;25:523–6.
[72] Ozan O, Turkyilmaz I, Ersoy AE, McGlumphy EA, Rosenstiel SF. Clinical accuracy of 3 different types of computed tomography-derived stereolithographic surgical guides in implant placement. J Oral Maxillofac Surg 2009;67:394–401.
[73] Griffith LG, Naughton G. Tissue engineering–current challenges and expanding opportunities. Science 2002;295:1009–14.
[74] Yamaoka T, Tabata Y, Ikada Y. Distribution and tissue uptake of poly (ethylene glycol) with different molecular weights after intravenous administration to mice. J Pharm Sci 1994;83:1–6.

[75] He S, Timmer M, Yaszemski M, Yasko A, Engel P, Mikos A. Synthesis of biodegradable poly(propylene fumarate) networks with poly(propylene fumarate)–diacrylate macromers as crosslinking agents and characterization of their degradation products. Polymer (Guildf) 2001;42:1251–60.
[76] Zhang H, Hutmacher DW, Chollet F, Poo AN, Burdet E. Microrobotics and MEMS-based fabrication techniques for scaffold-based tissue engineering. Macromol Biosci 2005;5:477–89.
[77] Ott HC, Matthiesen TS, Goh S-K, Black LD, Kren SM, Netoff TI, et al. Perfusion-decellularized matrix: using nature's platform to engineer a bioartificial heart. Nat Med 2008;14:213–21.
[78] Song JJ, Guyette JP, Gilpin SE, Gonzalez G, Vacanti JP, Ott HC. Regeneration and experimental orthotopic transplantation of a bioengineered kidney. Nat Med 2013;19:646–651.
[79] Andersson H, van den Berg A. Microfabrication and microfluidics for tissue engineering: state of the art and future opportunities. Lab Chip 2004;4:98–103.
[80] Salgado AJ, Coutinho OP, Reis RL. Bone tissue engineering: state of the art and future trends. Macromol Biosci 2004;4:743–65.
[81] Healy KE, Guldberg RE. Bone tissue engineering. J Musculoskelet Neuronal Interact 2007;7:328–30.
[82] Heller C, Schwentenwein M, Russmueller G, Varga F, Stampfl J, Liska R. Vinyl esters: low cytotoxicity monomers for the fabrication of biocompatible 3D scaffolds by lithography based additive manufacturing. J Polym Sci Part A-1: Polym Chem 2009;47:6941–54.
[83] Lu Y, Mapili G, Suhali G, Chen S, Roy K. A digital micro-mirror device-based system for the microfabrication of complex, spatially patterned tissue engineering scaffolds. J Biomed Mater Res A 2006;77:396–405.
[84] Ovsianikov A, Deiwick A, Van Vlierberghe S, Dubruel P, Möller L, Dräger G, et al. Laser fabrication of three-dimensional CAD scaffolds from photosensitive gelatin for applications in tissue engineering. Biomacromolecules 2011;12:851–8.
[85] Schüller-Ravoo S, Teixeira SM, Feijen J, Grijpma DW, Poot AA. Flexible and elastic scaffolds for cartilage tissue engineering prepared by stereolithography using poly(trimethylene carbonate)-based resins. Macromol Biosci 2013;13:1711–9.
[86] Naumann A, Aigner J, Staudenmaier R, Seemann M, Bruening R, Englmeier KH, et al. Clinical aspects and strategy for biomaterial engineering of an auricle based on three-dimensional stereolithography. Eur Arch Otorhinolaryngol 2003;260:568–75.
[87] Hwang NS, Kim MS, Sampattavanich S, Baek JH, Zhang Z, Elisseeff J. Effects of three-dimensional culture and growth factors on the chondrogenic differentiation of murine embryonic stem cells. Stem Cells 2006;24:284–91.
[88] Novosel EC, Kleinhans C, Kluger PJ. Vascularization is the key challenge in tissue engineering. Adv Drug Deliv Rev 2011;63:300–11.
[89] Chan V, Jeong JH, Bajaj P, Collens M, Saif T, Kong H, et al. Multi-material bio-fabrication of hydrogel cantilevers and actuators with stereolithography. Lab Chip 2012;12:88–98.
[90] Sodian R, Loebe M, Hein A, Martin DP, Hoerstrup SP, Potapov EV, et al. Application of stereolithography for scaffold fabrication for tissue engineered heart valves. ASAIO J 2002;48:12–6.
[91] Hockaday LA, Kang KH, Colangelo NW, Cheung PY, Duan B, Malone E, et al. Rapid 3D printing of anatomically accurate and mechanically heterogeneous aortic valve hydrogel scaffolds. Biofabrication 2012;4:035005.
[92] Jeong JH, Chan V, Cha C, Zorlutuna P, Dyck C, Hsia KJ, et al. "Living" microvascular stamp for patterning of functional neovessels; orchestrated control of matrix property and geometry. Adv Mater 2012;24:58–63. 1.
[93] Hsieh TM, Ng CWB, Narayanan K, Wan ACA, Ying JY. Three-dimensional microstructured tissue scaffolds fabricated by two-photon laser scanning photolithography. Biomaterials 2010;31:7648–52.
[94] Melissinaki V, Gill AA, Ortega I, Vamvakaki M, Ranella A, Haycock JW, et al. Direct laser writing of 3D scaffolds for neural tissue engineering applications. Biofabrication 2011;3:045005.
[95] Arcaute K, Mann B, Wicker R. Stereolithography of spatially controlled multi-material bioactive poly(ethylene glycol) scaffolds. Acta Biomater 2010;6:1047–54.
[96] Mirsaidov U, Scrimgeour J, Timp W, Beck K, Mir M, Matsudaira P, et al. Live cell lithography: using optical tweezers to create synthetic tissue. Lab Chip 2008;8:2174–81.
[97] Bajaj P, Marchwiany D, Duarte C, Bashir R. Patterned three-dimensional encapsulation of embryonic stem cells using dielectrophoresis and stereolithography. Adv Healthc Mater 2012;2:450–458.
[98] Deforest CA, Anseth KS. Cytocompatible click-based hydrogels with dynamically tunable properties through orthogonal photoconjugation and photocleavage reactions. Nat Chem 2011;3:925–31.
[99] Chan V, Park K, Collens MB, Kong H, Saif TA, Bashir R. Development of miniaturized walking biological machines. Sci Rep 2012;2:1–8.